

UT-GOM2-1 Hydrate Pressure Coring Expedition

Chapter 2. Expedition Methods

Contents

| | |
|--|----|
| Chapter 2. Expedition Methods | 3 |
| 2.1 Introduction | 3 |
| 2.1.1 Determining Hole Locations | 3 |
| 2.1.2 Drilling and Coring..... | 4 |
| 2.1.3 Depth References | 7 |
| 2.1.4 Methane Hydrate Stability Zone..... | 8 |
| 2.1.5 Core Handling | 9 |
| 2.1.6 Abbreviations and acronyms | 9 |
| 2.1.7 Data Storage and References | 12 |
| 2.2 Rig Instrumentation | 13 |
| 2.3 Pressure Coring | 14 |
| 2.3.1 Pressure Coring Tool with Ball Valve (PCTB)..... | 14 |
| 2.3.2 PCTB operation | 18 |
| 2.3.3 PCTB monitoring | 19 |
| 2.4 Physical Properties and Core Transfer | 20 |
| 2.4.1 Pressure Core | 20 |
| 2.4.2 Depressurized Whole Core XCT | 23 |
| 2.5 Quantitative Degassing | 23 |
| 2.6 Lithostratigraphy..... | 26 |
| 2.6.1 Lithostratigraphic nomenclature | 26 |
| 2.6.2 Visual Core Description..... | 26 |
| 2.6.3 Smear slide description..... | 28 |
| 2.6.4 Laser diffraction particle size analysis | 29 |
| 2.6.5 Mineralogy | 29 |
| 2.7 Geochemistry and Microbiology..... | 29 |
| 2.7.1 Pressure core gases..... | 29 |
| 2.7.2 Sedimentary gases | 30 |
| 2.7.3 Pore water | 30 |
| 2.7.4 Microbiology | 33 |
| 2.8 Wireline Logging..... | 33 |
| 2.8.1 Tools description..... | 34 |
| 2.8.2 Log Data Quality..... | 37 |
| 2.9 References..... | 38 |

List of Figures

| | |
|---|----|
| Figure 2.1.1 The bottom hole assembly (BHA) schematic of the PCTB cutting shoe configuration..... | 5 |
| Figure 2.1.2 The bottom hole assembly (BHA) schematic of the PCTB face bit configuration..... | 6 |
| Figure 2.1.3 PCTB face bit (left) and PCTB cutting shoe (right) configurations of the drill bit. | 7 |
| Figure 2.1.4 Reference depth definitions (see Table 2.1.1 for nomenclature)..... | 8 |
| Figure 2.1.5 Map of the expedition data directory for H002..... | 12 |
| Figure 2.3.1 Schematics and Drawing of the PCTB-CS. | 15 |
| Figure 2.3.2 Images and schematics of the PCTB-CS BHA and PCTB-FB. | 17 |
| Figure 2.3.3 Photo showing the half -open ball valve sealing mechanism in the PCTB..... | 18 |
| Figure 2.5.1 Photo of Geotek degassing manifolds and volume measuring equipment. | 24 |
| Figure 2.5.2 Schematic of Geotek degassing manifolds and volume measuring equipment..... | 25 |
| Figure 2.6.1 Shepard classification scale (Shepard, 1954). | 27 |
| Figure 2.8.1 Wireline logging tool string deployed in Hole GC 955 H002..... | 35 |

List of Tables

| | |
|--|----|
| Table 2.1.1 List of the expedition abbreviations and acronyms. | 11 |
| Table 2.2.1 Parameters acquired as function of time during drilling and coring operations..... | 14 |
| Table 2.3.1 List of Parameters collected during PCTB operation. | 20 |
| Table 2.7.1 Treatment and storage of squeezed pore water samples. | 32 |
| Table 2.8.1 Logging tools used with Specifications..... | 36 |
| Table 2.8.2 Acronyms and units used for downhole wireline tools, data, and measurements. | 36 |

Chapter 2. Expedition Methods

Abstract

This chapter documents the procedures and methods employed by the UT-GOM2-1 Expedition on the Helix *D/V Q-4000* vessel; dockside at the demobilization dock, InterMoor, Port Fourchon, LA; and during subsequent limited shore-based analyses. Dockside analyses reported here include continued pressure core logging, curation, quantitative degassing, gas analysis, and mud lab activities. The limited shore-based analyses reported here include initial core scanning and core description at Ohio State University, smear slide and visual descriptions at the University of New Hampshire, and geochemical analyses at the University of Washington. All work discussed was completed between June and September 2017. Future shore-based analyses of UT GOM2-01 results will be described in separate individual publications. This expedition report is modeled after the reporting style of the International Ocean Discovery Program (IODP). The methods used during the expedition were designed to conform to IODP protocols as much as possible.

2.1 Introduction

This introductory section provides an overview of vessel operations, depth scale terminology, curatorial conventions, general core handling and analyses, report nomenclature, and expedition data storage.

2.1.1 Determining Hole Locations

UT-GOM2-1 drilled two deep stratigraphic test wells in the Gulf of Mexico in the Green Canyon 955 (GC 955) protraction block located 232 kilometers south of Port Fourchon, Louisiana, USA: 1) Hole GC 955 H002 (H002) and Hole GC 955 H005 (H005).

The vessel position was determined by GPS using a WinFrog system (Fugro's integrated navigation software). DGPS1, differential DPS, was used and therefore the accuracy of the WinFrog position is typically less than 1 meter.

One Compatt seafloor transponder was placed on the seafloor. With one transponder, the peak radial difference is 14.9 m. Thus the actual hole position could lie anywhere within a circle of 14.9 m radius around the estimated position.

The process to determine the location of the drilled hole was as follows.

- 1) Q4000 arrived on location
- 2) Performed as found survey and lay seafloor transponder
- 3) Located original H001 well drilled in 2009
- 4) Placed marker in H001 location
- 5) The planned well was located based on a specified direction and distance from H001
- 6) A marker was placed on the planned well location
- 7) The drill string was then run to just above the seafloor
- 8) The vessel was positioned over the marker on seabed

4 UT-GOM2-1 Hydrate Pressure Coring Expedition

- 9) The drill string position was confirmed by having the ROV fly to the drill string and verify position on WinFrog

2.1.2 Drilling and Coring

The pressure coring tool with ball valve in the cutting shoe configuration (PCTB-CS) and the pressure coring tool with ball valve in the face bit configuration (PCTB-FB) were deployed on UT-GOM2-1 (Section 2.3 Pressure Coring). To core, the PCTB core barrel is lowered by wireline and latched into the bottom hole assembly (BHA). Then the drill pipe is advanced while rotating for the interval to be cored (up to 10 ft). To drill without coring, a center bit replaces the PCTB core barrel inside the BHA. During UT-GOM2-1, pressure coring was undertaken for targeted intervals and when not coring the hole was advanced with the center bit in place.

The PCTB-CS and the PCTB-FB require different bottom hole assemblies. The BHA for the PCTB-CS consists of a drill bit with an outer diameter of 9 $\frac{7}{8}$ inches (250.8 mm) and an inner diameter of 3 $\frac{1}{2}$ inches (96.5 mm), one stabilized bit sub, one seal bore drill collar, one landing saver sub, one modified top sub, one modified head sub, one 9 $\frac{7}{8}$ inch stabilizer, one 8 $\frac{1}{2}$ inch (215.9 mm) drill collar, one 9 $\frac{7}{8}$ inch stabilizer, four 8 $\frac{1}{2}$ inch drill collars, and one crossover sub (Figure 2.1.1). The PCTB-FB BHA (Figure 2.1.2) differs from the PCTB-CS only in the drill bit used. The PCTB-FB drill bit has a 9 $\frac{7}{8}$ inch outside diameter and a 2 inch (5.08 cm) inside diameter. As a result, when running the PCTB-CS BHA other coring and logging tools can be used, but when running the PCTB-FB BHA other tools cannot be used. A comparison of the drill bits is shown in Figure 2.1.3. See 2.3 Pressure Coring for more information.

The drilling plan called for drilling to approximately 1000 fbsf with seawater and occasional gel sweeps. At depths greater than this, the initial plan was to continuously use weighted mud, up to 10.5 ppg, during all drilling and coring. The purpose of the weighted mud was to provide improved hole cleaning, improved hole stability, and to balance against any overpressure (gas or water) that might be present. Liquid bentonite-based mud (16.0 ppg) was supplied by MI SWACO of Schlumberger. The 16.0 ppg mud was cut back to the desired weight and viscosity onboard the vessel. Two MI-SWACO mud engineers were onboard throughout the expedition to oversee the mud program.

Before drilling, the ROV performed an as found seafloor survey. During drilling, an ROV was used to continuously monitor the wellbore for any evidence of water or gas flow. After the hole was completed, the ROV performed an as left seafloor survey.

After completion of the scientific program, the well was abandoned according to the permitted procedure determined by BSEE. Abandonment included the placement of a cement plug at least 300 ft. The integrity and final location of the cement was verified by applying drill string weight after it had set. A Schlumberger cementing engineer was onboard throughout the expedition to oversee the cementing program.

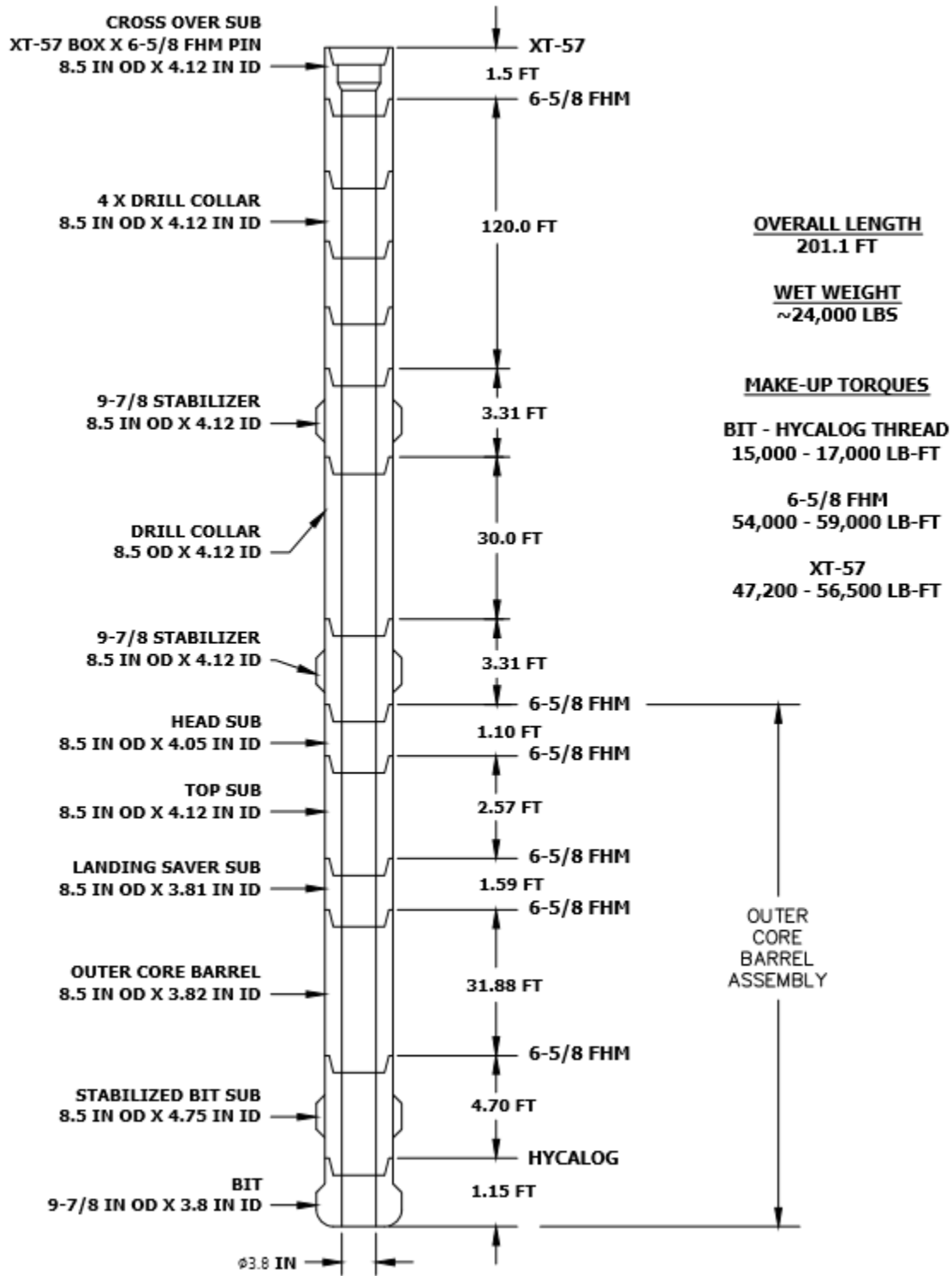


Figure 2.1.1 The bottom hole assembly (BHA) schematic of the PCTB cutting shoe configuration.

6 UT-GOM2-1 Hydrate Pressure Coring Expedition

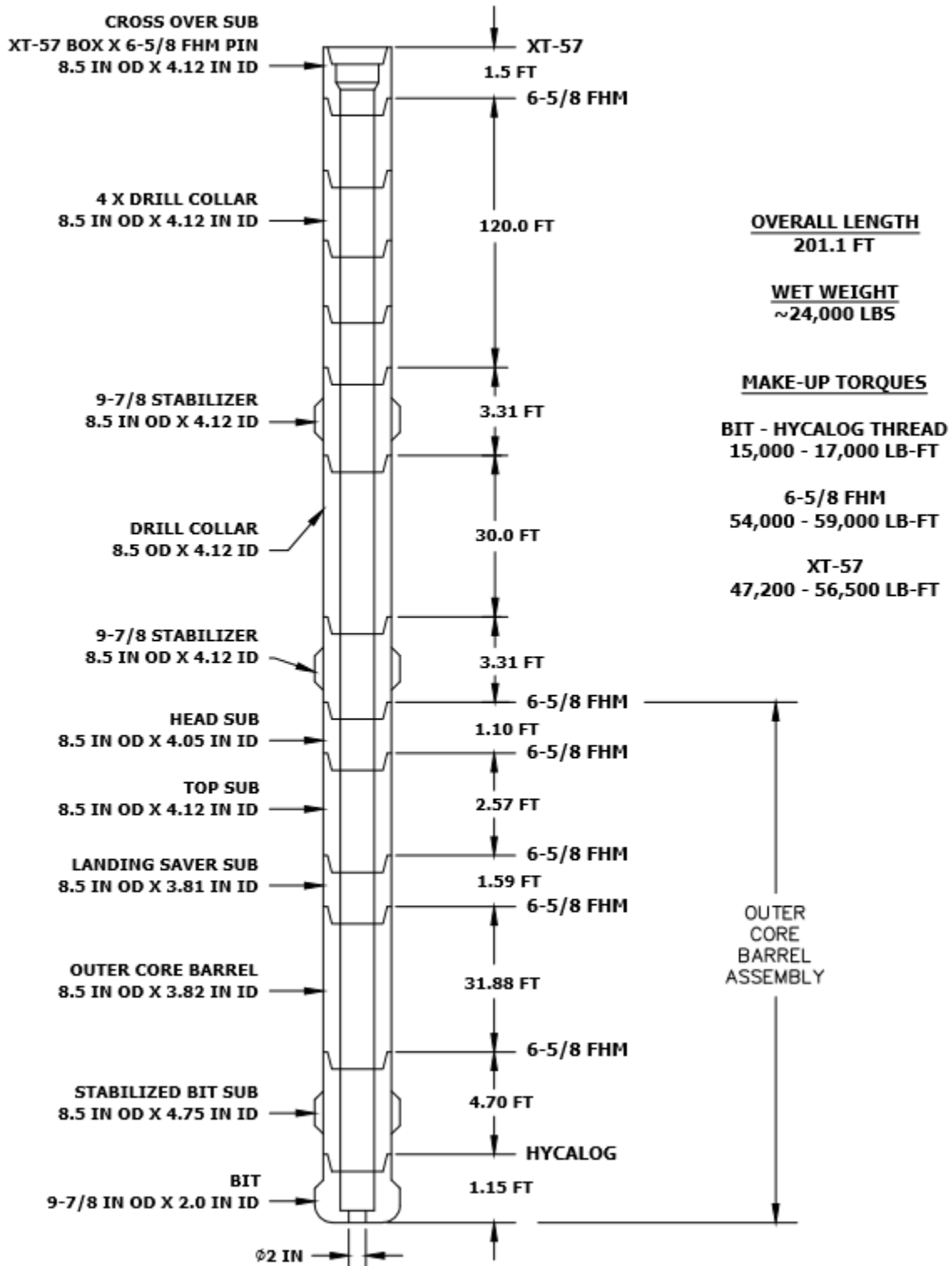


Figure 2.1.2 The bottom hole assembly (BHA) schematic of the PCTB face bit configuration.

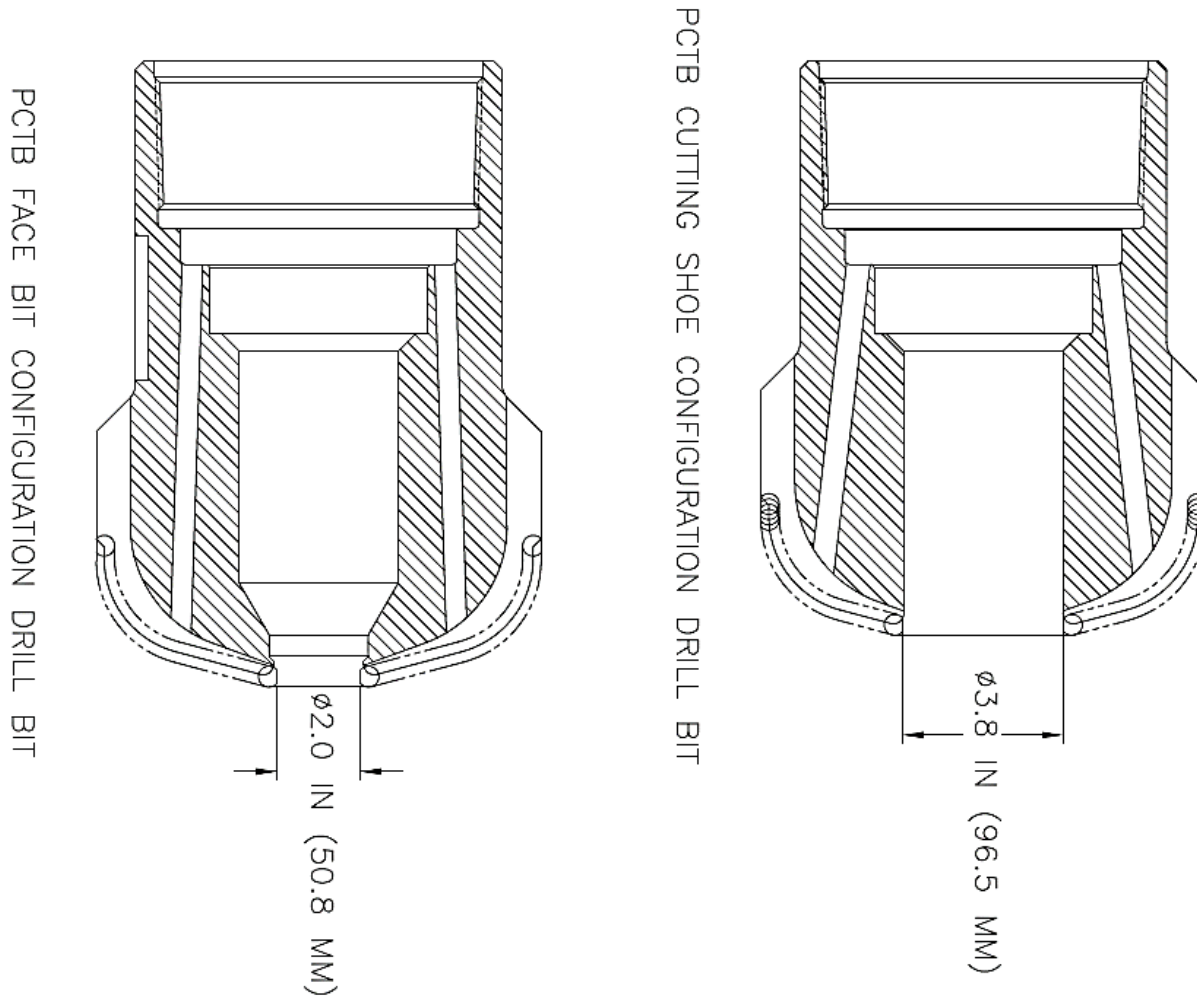


Figure 2.1.3 PCTB face bit (left) and PCTB cutting shoe (right) configurations of the drill bit.

2.1.3 Depth References

Personnel on the *D/V Q4000* operate in decimal feet. Drilling and core depths were measured initially in terms of feet below rig floor (fbrf) to streamline communications and reduce potential for error. From these values, depths in meters below seafloor (mbsf) were calculated by first converting to metric units and subtracting the water depth measured from the rig floor at each hole location. For this purpose, water depth was determined by measuring drilling depth in fbrf to the mud line as observed by the remotely operated underwater vehicle (ROV) as the drill bit tagged the seafloor for both holes established in this project. Core top measurements in mbsf were determined by subtracting the seafloor depth from the core top depth (mbrf) (Figure 2.1.4). The core top mbsf measurement is the ultimate depth reference for all core-related depth calculations. In this report, data continue to be reported in fbrf for information related directly to operations, pressure core deployment and recovery. For scientific publications and communication, however, the most common units are mbsf. This transition was started by reporting well logging data and data collected on the pressure cores in both fbrf and mbsf.

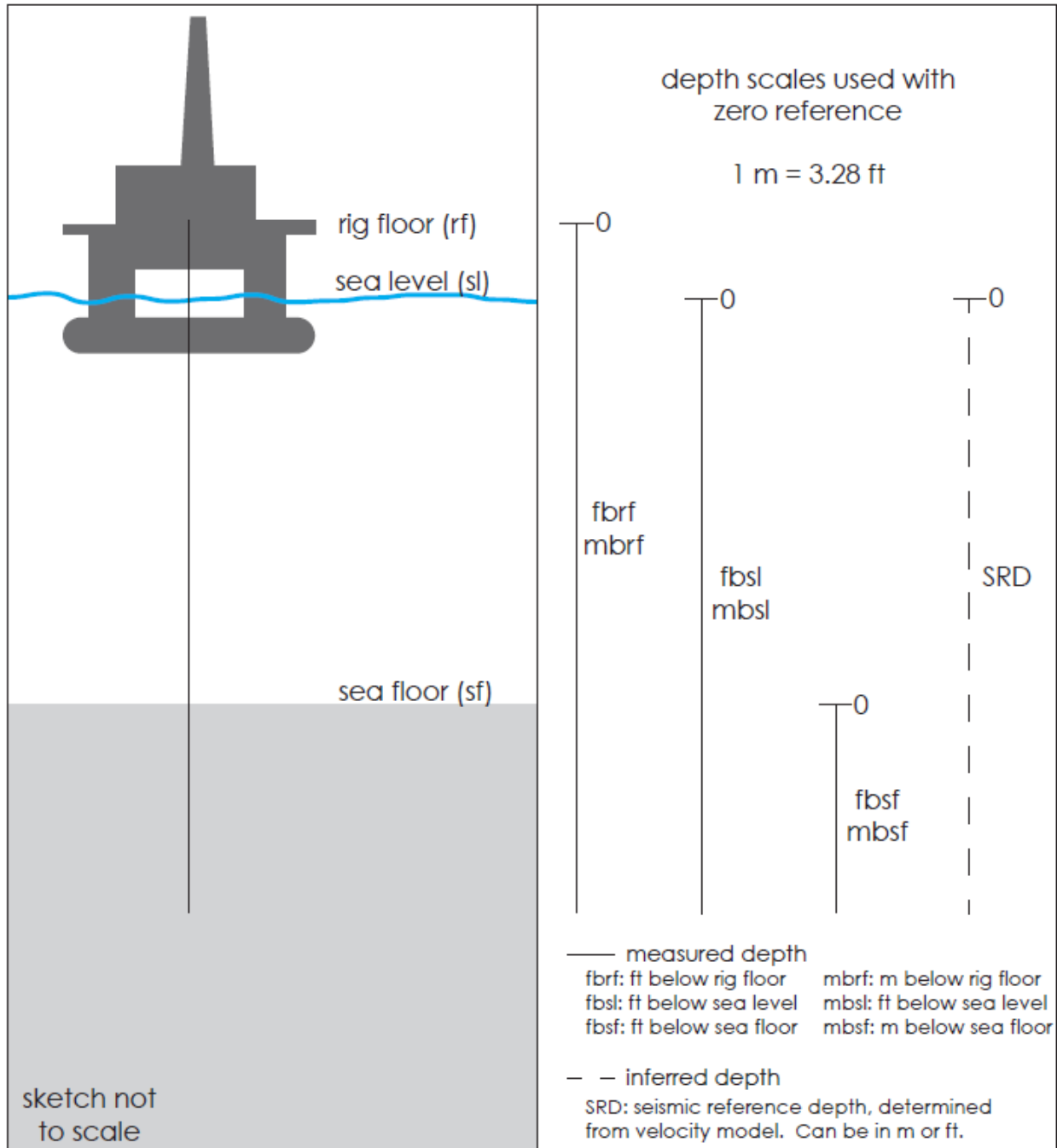


Figure 2.1.4 Reference depth definitions (see Table 2.1.1 for nomenclature).

2.1.4 Methane Hydrate Stability Zone

In this expedition report the methane hydrate stability zone was defined as the region of pressure and temperature where methane hydrate is stable at seawater salinity (3.5 wt% NaCl). And, the methane hydrate stability boundary as the pressure and temperature conditions when methane hydrate at seawater salinity transitions from being stable to unstable.

2.1.5 Core Handling

As pressure cores arrived on deck, they were chilled in a cold shuck and then craned to Geotek's Pressure Core Analysis and Transfer System (PCATS). Because the PCATS full characterization can take 12 hr or longer, the pressure core was first characterized in PCATS with an initial (4-6 hr) characterization which was completed before the next pressure core arrived from the rig floor. After the initial characterization, pressure cores were shuttled to temporary storage pending full characterization at a later time.

Unlike previous hydrate pressure coring expeditions, of longer duration, UT-GOM2-1 did not have enough time between coring H002 and H005, nor after H005, to complete the full characterization of all the pressure cores acquired. Thus it was planned that PCATS would be remobilized at Port Fourchon, just after demobilization from the vessel, and the full characterization completed at that time. (See Section 2.4 Physical Properties for a full description of the analytical methods used in the initial and full characterization.)

Plans for the sectioning and allocation of pressure core were drafted on the initial characterization and finalized just before cutting. Sections of core were identified for transport to UT, slow degassing (see Section 2.5 Quantitative Degassing), or rapid depressurization. Depressurized samples, from unsuccessful pressure coring runs, rapid depressurization in PCATS, or slow quantitative degassing, were processed for sedimentological (see Section 2.6 Lithostratigraphy) and geochemical analyses (see Section 2.7 Geochemistry) in the UT-GOM2-1 mud lab.

The complete identification number for a sample and or data associated with a sample consists of the following information: expedition, hole, core number with PCTB coring configuration designation (CS or FB), and core section number. Thus UT-GOM2-1-H002-5CS-3 would represent the third section cut (3) from the top of a core taken during this expedition (UT-GOM2-1) during the fifth coring run (5) in H002 using PCTB-CS (CS).

2.1.6 Abbreviations and acronyms

All abbreviations and acronyms used in this this expedition report are listed in Table 2.1.1.

| Term | Definition |
|------------------|---|
| bbl, bbls | US oilfield barrel, barrels |
| BHA | Bottom hole assembly |
| BOEM | Bureau of Ocean Energy Management |
| BPM | Barrels per minute |
| BSEE | Bureau of Safety and Environmental Enforcement |
| BSR | Seismic bottom hole reflector |
| CS | Cutting shoe configuration of the PCTB |
| Cs | Cesium |
| CT | Computed tomography |
| Cu | Copper |
| <i>D/V Q4000</i> | Helix <i>D/V Q4000</i> deepwater well intervention vessel |
| DOE | Department of Energy |

| Term | Definition |
|-------------|---|
| DPS | Dynamic Positioning System |
| DST | Data storage tag |
| FB | Face bit configuration of the PCTB |
| fbrf | feet below rig floor |
| fbsf | feet below seafloor |
| fbsl | feet below sea level |
| gAPI | American Petroleum Institute units |
| GC | Green Canyon |
| GOM2 | Genesis of Methane Hydrates in Coarse-Grained Systems: Northern Gulf of Mexico also known as the DOE project Deepwater Methane Hydrate Characterization & Scientific Assessment, DE-FE0023919 |
| gpm | gallons per minute |
| H001 | Hole Green Canyon 955 H001 |
| H002 | Hole Green Canyon 955 H002 |
| H005 | Hole Green Canyon 955 H005 |
| hr | hour |
| HRLT | High-Resolution Laterolog Array Tool |
| HS | Headspace gas |
| I001 | Hole Green Canyon 955 I001 |
| IODP | Integrated Ocean Drilling Program |
| K | One Thousand (e.g. 30K = 30,000) or Potassium depending on context |
| KeV | kiloelectronvolts |
| klbs | Thousand pounds |
| LAS | Log ASCII standard |
| LDNR | Louisiana Department of Natural Resources |
| LWD | Logging while drilling |
| μA | microamps |
| m | Meter |
| mCi | microcurie unit of radioactivity |
| M | Molar |
| MBq | megabecquerel unit of radioactivity |
| mbrf | meters below rig floor |
| mbsf | meters below seafloor |
| mbsl | meters below sea level |
| MD | measured depth |
| mD | milli-Darci |
| Mpa | megapascal |
| NEPA | National Environmental Policy Act |
| NETL | National Energy Technology Laboratory |
| nmi | Nautical Mile |

| Term | Definition |
|-------------|--|
| OSU | Ohio State University |
| PCATS | Pressure core analysis and transfer system |
| PCC | UT Pressure Core Center |
| PCTB | Pressure coring tool with ball valve |
| PCTB-CS | PCTB in the cutting shoe configuration |
| PCTB-FB | PCTB in the face bit configuration |
| POOH | pull out of hole |
| ppb | parts per billion |
| ppg | pounds per gallon |
| ppm | parts per million |
| psi, psig | pounds per square inch, pounds per square inch by gauge |
| psu | practical salinity units |
| Q001 | Hole Green Canyon 955 Q001 |
| rabbit | core follower, deployed with a DST called the rabbit DST |
| rf | rig floor |
| ROP | Rate of penetration |
| ROV | Remotely Operated Underwater Vehicle |
| s | seconds |
| SEMS | Helix Safety and Environmental Management System |
| SED | Particle size settling velocity data |
| sf | seafloor |
| sl | sea level |
| spud | start drilling the hole |
| spm | strokes per minute |
| stand | 2 joints of drill pipe screwed together |
| TD | Total depth |
| Th | Thorium |
| U | Uranium |
| USCG | United States Coast Guard |
| USEPA | United States Environmental Protection Agency |
| USGS | United States Geological Survey |
| UT | The University of Texas at Austin |
| UT-GOM2-1 | UT GOM2 Hydrate Pressure Coring Expedition 1 |
| WBM | Water-based mud |
| WGS84 | World Geodetic System 1984 |
| WOB | Weight on bit |
| wt% | percent by weight |

Table 2.1.1 List of the expedition abbreviations and acronyms.

2.1.7 Data Storage and References

All raw and processed data from the expedition will be stored in a web accessible data directory. Data files can be found in the data directory by chapter and hole as shown for H002 in Figure 2.1.5. All data plots in this and other chapters reference the file containing the data shown. Specific data set locations are also referenced in the text.

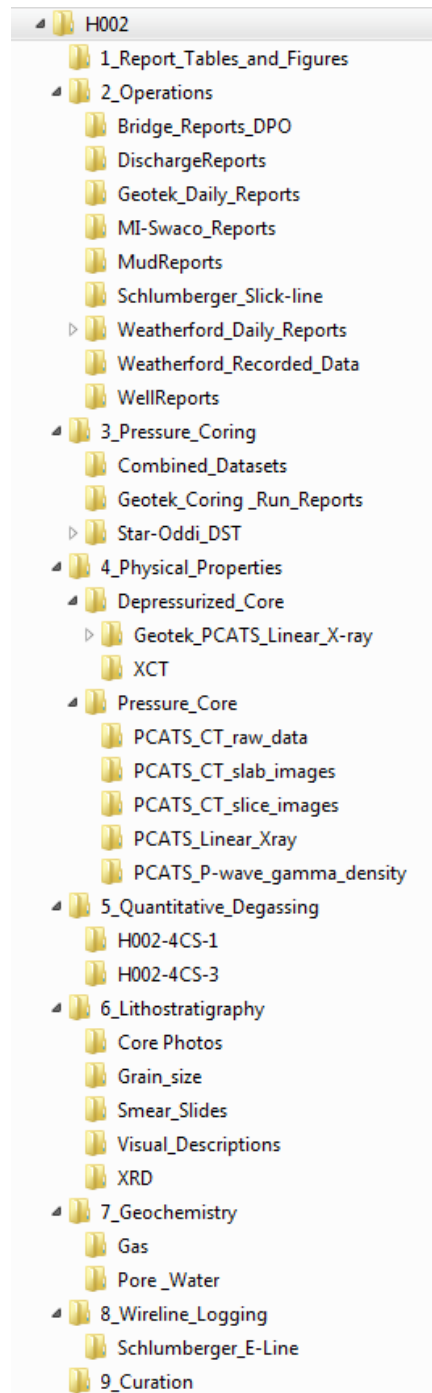


Figure 2.1.5 Map of the expedition data directory for H002.

2.2 Rig Instrumentation

We acquired data from four different rig locations: at the rig floor (which included all parameters related to the movement of drill pipe), at the pumps, on the slickline, and in the PCTB. The rig floor and pump data were acquired by sensors installed by Weatherford. Slickline data were recorded directly by the Schlumberger slickline unit. In the PCTB, pressure and temperature were monitored with Star-Oddi Centi-TD temperature depth recorders (data storage tags or DSTs). See summary Table 2.2.1 Parameters acquired as function of time during drilling and coring operations.

Weatherford installed all the necessary sensors and wiring prior to spudding hole H002. The data were routed to a central server then sent out to satellite CPUs at various locations on the vessel. This allowed for real time data viewing and data downloads. Once a day the Weatherford engineer would send out a data report, plots of the previous 24 hours of data, and a LAS file with the raw data for archive purposes. The slickline, which was used for deploying and retrieving the PCTB, was operated and monitored by Schlumberger. Data were collected every morning around 1 AM for the previous day of operations (0000 hr to 2359 hr). Weatherford LAS files and Schlumberger slickline data were archived and can be found in the expedition data directory as shown in Table 2.2.1.

In the PCTB, pressure and temperature were monitored in three locations. The rabbit DST was placed inside the core follower (or rabbit) that advanced up the liner as core material was added beneath it. As the rabbit was in the same environment as the sediment core, it provides the most representative record of the pressure-temperature history of the core (Figure 2.3.1A). As a backup, another DST was placed in a recess at the bottom of the inner tube plug. This plug DST was exposed to the same pressure as the Rabbit DST, but was in thermal contact with the body of the tool. Thus, the temperature fluctuations were more extreme and the temperature record should be used with care (Figure 2.3.1A). A third DST was placed in the core retrieval tool (pulling tool). This pulling tool DST measured the temperature and pressure within the borehole at the pulling tool depth. All temperatures and pressures were recorded in 10 second intervals and written to the DST internal memory. After the PCTB was recovered and the autoclave transferred to PCATS, rabbit and plug DSTs were retrieved and the data downloaded. Pulling tool DST data were downloaded at the end of the coring runs for each hole. DST data were archived and can be found in the expedition data directory as shown in Table 2.2.1.

All data were recorded in Universal Coordinated Time minus 5 hours (UTC-5) during operations at H002 and H005 except for Weatherford drilling data, which was behind UTC-5 by 3 minutes and 4 seconds during H002 only. This error was corrected between H002 and H005, such that all parameters for H005 were correctly recorded at UTC-5. All plotted Weatherford data from H002 in this report were offset to match UTC-5.

All available Weatherford coring data were combined with Schlumberger slickline, Geotek rabbit DST, and Geotek pulling tool DST data from the same time frame. Plots including slickline depth, slickline tension, pressure inside and outside the PCTB, core temperature, weight on bit, rate of penetration, and combined flow rate as a function of time were created for each hole and core and are shown in corresponding chapters (see Sections 3.3 and 4.3 Pressure Coring). All combined data files can be found

in the data directory under Pressure Coring / Combined Datasets. See the readme file located there for more direction.

| Parameter | Method of data acquisition | Data set | |
|-------------------------------------|---|--|-------------------------------------|
| Hook load | Direct measurement via sensor or transducer (4-20 mA) | Operations / Weatherford recorded data | |
| RPM | | | |
| Torque | | | |
| Standpipe pressure | | | |
| Hook position | | | |
| Block height | | | |
| Pump 1 and 2 rate | | | |
| Pump 3 rate | Recorded output from Schlumberger cement pump | | |
| Rate of penetration (ROP) | Calculated by Weatherford from two or more parameters above | | |
| Weight on bit (WOB) | | | |
| Hole depth | | | |
| Bit depth | | | |
| Flow in (all pump rates combined) | Recorded directly by the slickline unit | | Operations / Schlumberger slickline |
| Depth | | | |
| Tension | | | |
| Tension spike | | | |
| Speed | | | |
| Alarm status | | | |
| Pressure in the PCTB rabbit | Recorded by Data Storage Tags | Pressure Coring / Star_Oddi_DST | |
| Temperature in the PCTB rabbit | | | |
| PCTB inner tube plug pressure | | | |
| PCTB inner tube plug temperature | | | |
| Borehole (pulling tool) pressure | | | |
| Borehole (pulling tool) temperature | | | |

Table 2.2.1 Parameters acquired as function of time during drilling and coring operations.

2.3 Pressure Coring

Pressure coring was used to collect all cores during UT-GOM2-1. Pressure coring acquires samples at or near in situ pressure by sealing the core inside the coring autoclave immediately after the core has been cut. During UT-GOM2-1, pressure cores were collected using the DOE Pressure Coring Tool with Ball valve (PCTB).

2.3.1 Pressure Coring Tool with Ball Valve (PCTB)

The pressure coring tool with ball valve (PCTB) is a wireline coring system designed to recover core samples while maintaining the core at pressure within the methane hydrate stability zone. As discussed

in 2.1.2 Drilling and Coring, there are two optional PCTB cutting bit configurations: the cutting shoe (PCTB-CS, Figure 2.3.1 and Figure 2.3.2) and the face bit (PCTB-FB, Figure 2.3.2). During UT-GOM2-1, the PCTB-CS was tested in H002 and PCTB-FB in H005.

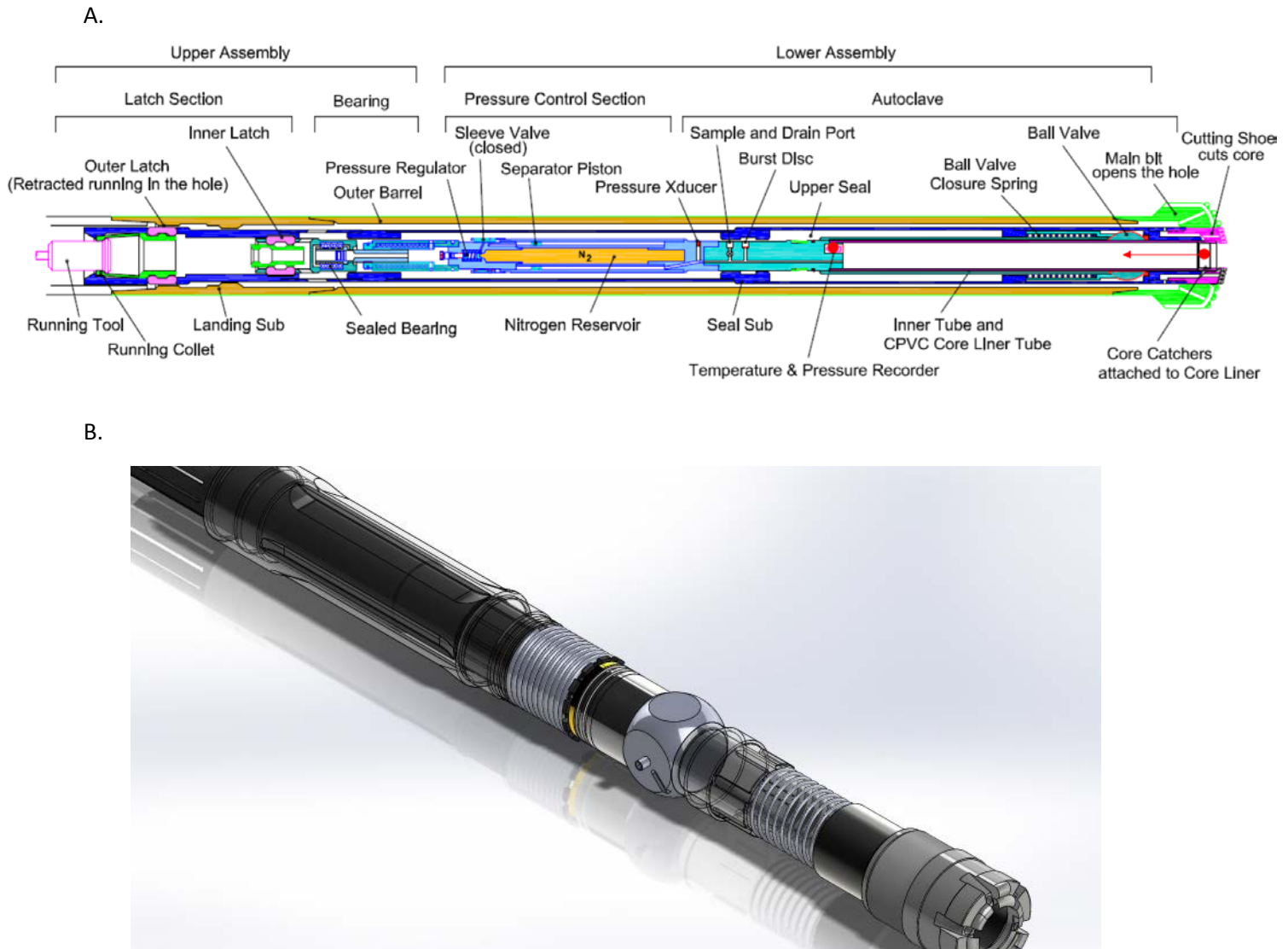


Figure 2.3.1 Schematics and Drawing of the PCTB-CS. A. Schematic of the PCTB-CS. Red dots show DST locations within the tool: one in the plug at the top of the autoclave immediately above the inner tube (plug DST), and one in the core follower (rabbit DST).

B. Drawing of Bottom end of the lower section of the PCTB with the cutting shoe configuration.

The PCTB tool runs in a drill pipe with a minimum inner diameter of $4\frac{1}{8}$ inches and collects cores that are nominally 51 mm (~2 inches) in diameter, contained in a plastic liner with outer diameter 59.4 mm (2.34 inches), and up to 3 m (~10 ft) long. It is rated to recover cores at pressures of up to 35 MPa (~5000 psi)

and uses a powered ball valve closure mechanism for rapid actuation and closure of the core barrel (Figure 2.3.3).

Wireline coring enables continuous pressure coring to take place using multiple core barrels (autoclaves) and alleviates the need to trip pipe. As shown in Figure 2.3.1A, the PCTB is composed of two assemblies: the lower assembly that collects the core and retains pressure; and the upper assembly that contains the BHA landing shoulder and the wireline latching interface.

The lower assembly in turn is composed of two sections: the autoclave and the pressure control section. The autoclave houses the core inner tube and top sealing ball valve. Each autoclave was equipped with a sample and drain port, and a 5,000 psi (34.5 MPa) burst disk. Should pressure build up in the autoclave, the burst disk will rupture. There is also an integral pressure transducer for monitoring the autoclave internal pressure once the tool is on deck and an autoclave pressure relief valve, integral to the tool, which can be operated manually but is not designed for degassing. Core catchers (outside diameter 60.3 mm or 2.375 inches) used on the end of the plastic liner act as one-way valves, letting core enter the liner while advancing the hole, but retaining core material when the PCTB is recovered to surface. The pressure control section provides a nitrogen-charged pressure-regulated system to maintain pressure on the autoclave after the core is cut and the ball is closed. The nitrogen in the pressure section remains separate from the core in the autoclave and only fluid pressure is transmitted between the sections. The upper and lower assemblies are combined to make up the complete tool at the drill floor.

The BHA hosts the main drilling bit and mechanisms to lock the coring tools in place. The PCTB-CS uses an extended cutting shoe that protrudes through the main bit at the base of the BHA (Figure 2.3.2). The extended cutting shoe acts as a pilot bit to cut and trim the core ahead of the main bit. In the PCTB-FB the main bit on the BHA advances the hole while cutting the core at the same time. Although the PCTB-CS inner core barrel is locked into the BHA in order to transmit torque to the cutting shoe, the inner tube and plastic core liner assembly is suspended on a bearing freeing the core liner to not rotate relative to the formation, to minimize core disturbance. The PCTB-FB inner core barrel is not locked into the rotation of the BHA. Instead the BHA rotates around it.

The PCTB version used on this expedition (the DOE PCTB modified by Geotek; also referred to by Geotek as the Geotek PCTB III) had a number of modifications designed to provide more reliable pressure retention and improved core recovery. These changes are discussed in the GOM2 Land Test Report (Flemings, 2016). Changes were made to internal flow paths, latch mechanisms, and internal ball closure timing mechanisms. Some details are also discussed in Flow testing below. There were four autoclaves, four pressure sections, and two upper assemblies on board.

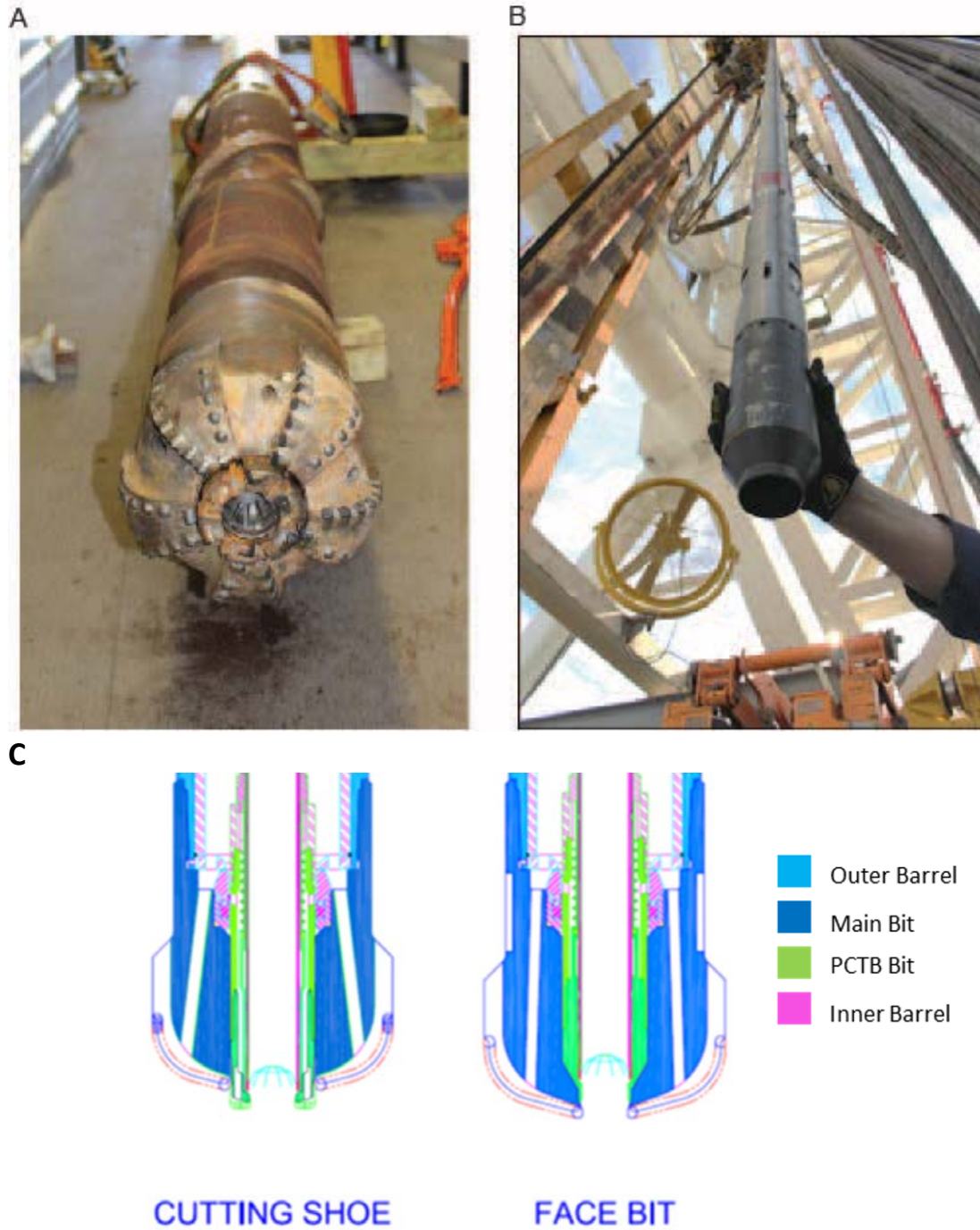


Figure 2.3.2 Images and schematics of the PCTB-CS BHA and PCTB-FB. A. The cutting shoe protrudes through the drill bit while latched in the BHA. , B. PCTB-FB inner barrel on the wireline at the GOM2 PCTB Land Test 1 (Flemings, 2016)., C. Enlarged Schematics of the PCTB-CS and PCTB-FB drill bits.



Figure 2.3.3 Photo showing the half-open ball valve sealing mechanism in the PCTB.

2.3.2 PCTB operation

The PCTB top and bottom assemblies were combined on the drill floor and deployed on the wireline with the running tool until the PCTB reached the bottom of the drill string and latched into the BHA. The bit was lowered to the bottom of the hole and coring commenced with the agreed drilling parameters (rate of penetration, weight on bit, pump rates). As the drill string was rotated, the PCTB advanced into the formation, cutting the core.

Recovery of the PCTB began as the BHA was lifted off the bottom of the hole. A pulling tool lowered on the wireline was used to latch onto the PCTB, which on lifting triggered the closing of the lower ball valve and the release of the nitrogen charge, sealing the core inside the autoclave. The nitrogen charge boost is designed to force water into the autoclave, increasing the pressure until the pressure inside is elevated above in situ hydrostatic pressure. This boost charge is designed to help align the seals to prevent slow leakage during recovery. If the boost charge has worked correctly, the pressure in the autoclave can exceed the in situ pressure on recovery. The pulling tool then released the outer latch that enables the complete PCTB assembly to be pulled to the surface. The PCTB was pulled to the rig floor where the upper assembly was removed and the lower assembly was immediately placed in a glycol-cooled cold shuck to ensure that the core remained inside methane hydrate stability zone.

After approximately 30 minutes in the cold shuck, the PCTB was removed to the service van where the autoclave was pressure-isolated and then separated from the pressure control section. At this point the pressure in the autoclave was measured for the first time. The autoclave was prepared for core transfer to PCATS by installing the PCATS adapter onto the autoclave. The autoclave was then moved to the PCATS laboratory, where the core was removed, analyzed, cut, and transferred to specialized pressure cells for analysis or transportation (see 2.4 Physical Properties and Core Transfer).

Flow testing

Previously, at high flow rates, differential pressure could build between the inside and outside of the core liner to levels sufficient to damage or collapse the liner. To reduce the chances of core liner collapse,

following the PCTB 2015 Land Test program (Flemings, 2016), the PCTB was modified using a flow diverter to ensure that all the fluid flow to the bit was diverted around the outside of the inner barrel. During this expedition, five flow tests were run prior to coring with the PCTB-CS) and an instrumented core liner to measure the relationship between flow rate and pressure differential across the core liner. The Instrumented Core Liner was equipped with six additional DSTs placed at inside and outside the liner at three locations lengthwise along the liner. Pressure differential was then calculated by the difference between the pressure outside and inside the liner. Pressure differentials were plotted for each flow rate. More details about the flow tests and flow test results can be found in Chapter 3, Section 3.3.1 Flow Tests.

Full Function tests

Full Function tests were conducted to test the ability of the tool to successfully collect and maintain a pressurized sample. During a Full function test the PCTB was operated as it would at the end of a typical coring run, except the test is run in the drill string above the formation. The goal is to collect seawater in the core liner in which the PCTB is actuated, the ball valve closes, and the fluid within the core liner remains pressurized back to the surface. All coring activity was plotted using the method described in Section 2.2 Rig Instrumentation above. More information about the Full function tests and test results can be found in Chapter 3, Section 3.3.2 Full Function Tests and Chapter 4, Section 4.3.2 Full Function Tests.

2.3.3 PCTB monitoring

As mentioned in Section 2.1.2 Drilling and Coring above, pressure and temperature were monitored in three locations with DSTs. Pressure and temperature data points from the DST rabbit (or plug DST data when rabbit DST data were not available) for each coring run were plotted against the methane hydrate stability boundary to determine if the PCTB exited the methane hydrate stability zone similar to the approach used during previous pressure coring expeditions (Collett et al., 2008; Inada and Yamamoto, 2015) during warming as the PCTB is raised through the thermocline and manipulated on deck. See Sections 3.3 and 4.3 Pressure Coring for all results.

All DST data files can be found by hole in the expedition data directory under Pressure Coring / Starr-Oddi DST. See the readme file located there for more direction.

For each coring run, Geotek LTD also record the data listed in Table 2.3.1. These data were archived in the Expedition Data Directory files under Curation.

| | |
|--|--|
| Core Log | Date |
| | Site |
| | Core # |
| Hardware (which tools are running and how they are configured) | Autoclave Number (A/C #) |
| | Pressure Section Configuration (Pres Sect #) |
| | Upper Section Configuration (Up Sect #) |
| | Reservoir Pressure (psi) |
| | Reservoir Pressure (MPa) |
| | Set/Boost Pressure (psi) |
| | Set/Boost Pressure (MPa) |
| | Plug DST ID number |
| | Rabbit DST ID number |
| | Cored Location / Depth |
| Water depth (m) | |
| Depth below rig floor (m) | |
| Pressure and Temperature Data | In situ Pressure (MPa) recorded by plug and rabbit DSTs |
| | Recovery Pressure (psi and MPa) recorded by plug and rabbit DSTs |
| Coring and Processing Time | Date into pipe |
| | Time into pipe |
| | Total Time in pipe (hrs) |
| | Date in PCATS |
| | Time in PCATS |
| Core Recovery | Cored Interval (m) |
| | Total curated length (m) |
| | % Recovery of Cored Interval |
| Drilling Parameters from the rig floor | Drill String Rotation (RPM) |
| | Pump Rate (L/min) |
| | Weight on Bit (T) |
| | Pull-out Force (T) |
| | Rate of Penetration (m/h) |

Table 2.3.1 List of Parameters collected during PCTB operation.

2.4 Physical Properties and Core Transfer

2.4.1 Pressure Core

The Pressure Core Analysis and Transfer System (PCATS; (Schultheiss et al., 2014; Schultheiss et al., 2011)) was used to perform preliminary characterization of the cores. This characterization included X-ray imaging, P-wave velocity and gamma density core logs. Cores were sub-sectioned inside PCATS and transferred into storage chambers for either quantitative degassing or long term storage and transportation to the University of Texas at Austin. All pressure cores were logged twice in PCATS; an initial scan was conducted while onboard the *D/V Q-4000* and a final scan was performed at the post

expedition processing facility at Port Fourchon, Louisiana. The first scan was primarily used to develop a core cutting plan but the second scan should be used as the primary data set for interpretation. The P-wave and gamma density were logged at a spatial resolution of 0.5 cm. Because the P-wave and gamma density were collected on separate scans to the X-ray images or CT data sets, there is the potential for slight errors in down core registration of these data sets if core physically moved between scans. Where these errors have become egregious, they are noted in the report.

PCATS gamma density

Gamma density was calculated from the attenuation of a collimated beam of monochromatic gamma photons from a nominal 10 mCi (370 MBq) Caesium-137 (^{137}Cs) source (Schultheiss et al., 2011). This source was active enough to penetrate both the core and the aluminum pressure housing (wall thickness of 11 mm), and was shielded in lead with a rotating lead shutter (5mm diameter collimator). Calibration of gamma attenuation to gamma density, and from there to bulk density, relied on a set of standards of known average bulk density. The standards of choice for calibration of gamma attenuation to gamma density in standard sediments (water-saturated aluminosilicates) are aluminum and water of known thicknesses inside core liner. This results in similar electron density in the calibration pieces and the core, allowing gamma density and bulk density to track each other with high precision, though the resultant data were technically reported as gamma density rather than bulk density. Gamma counts averaged near 20000 (total counts) with an integration time of 5 seconds, making the error in the gamma density 1.4% (95% confidence interval).

Gamma density artifacts

The major artifact in the gamma density as collected during UT-GOM2-1 and presented in the field data set (30-June-2017) is due to the variation in the diameter of the acquired core. The calculation of gamma density performed in the field assumed that the core was of a constant diameter, which was not the case. The gamma density could be improved by reprocessing the data, using the X-ray CT data to constrain the diameter.

All gamma density data can be found by hole in the expedition data directory under Physical Properties / Pressure Core / PCATS P-wave gamma density /.

PCATS P-wave Velocity

Ultrasonic P-wave velocity was measured with a pulse transmission technique. The two 500 kHz acoustic transducers were mounted inside the aluminum pressure housing, perpendicular to the core axis (Schultheiss et al., 2011). The transducers were also perpendicular to but co-located along the core with the gamma ray beam. The P-wave velocity was calculated from the pulse travel time across the core material and the internal diameter of the core liner ultrasonic velocity with a precision of $\pm 1.5 \text{ m s}^{-1}$ and an accuracy of approximately $\pm 5 \text{ m s}^{-1}$. The pulse travel time across the core material is calculated by subtracting the travel time offset, which is the time required for the pulse to transit the core liner as well as the pressurizing fluid between the transducers and the core liner at a given temperature.

P-wave velocity artifacts

As with the gamma density, the major artifact in the P-wave data stems from the variations in core diameter. Again, as with the density, the data could be improved by reprocessing the travel time using CT-derived core diameters.

All p-wave data can be found by hole in the expedition data directory under Physical Properties / Pressure Core / PCATS P-wave gamma density /.

PCATS 2D and 3D X-ray

X-ray images were collected using a variable intensity, microfocal X-ray source and a digital flat-panel detector (Schultheiss et al., 2011). The source energy used was 120 keV at 400 μ A. The combination of microfocal source and high resolution flat-panel detector enabled images to be collected in PCATS with a 112 μ m/pixel resolution. Linear 2D X-rays were acquired using a continuous scanning technique providing a single line scan image of the complete core. X-ray CT data was collected on all the pressure cores at the same voxel resolution (112 μ m per side). These data sets were collected using multiple rotations along the length of the core. Each core rotation was 6.7 cm long and contained 400 images (0.8° increments).

The 2D X-ray linear image raw data file are 16-bit TIFF and have companion XML files containing information regarding the image collection. JPGs of each core were created and mathematically corrected for the variable thickness across the round core (virtually slabbed). 3D X-ray CT data sets are in individual folders as a stack of 16-bit TIFF files with a WholeCoreRecon.TXT file containing information regarding the CT stack. Two CT slabs perpendicular to each other along the axis of the core are provided as JPG files; these slabs are 5mm thick unless otherwise marked and taken slightly off center. Note that in all X-ray images provided by Geotek, the images are positive meaning denser objects which obscure the X-ray beam are darker than less dense material.

X-ray artifacts

X-ray images record the attenuation of a polychromatic X-ray beam as it passes through a sample. Attenuation at any given energy is a function of the thickness, density, and atomic number of a material, and because of this, attenuation of polychromatic X-rays by material of varied atomic number should not be used as a simple proxy for density. For instance, the drilling mud used on UT-GOM2-1 contained barite, and in the X-ray images the mud appears disproportionately dark—because its attenuation coefficient is far larger than that for silica or clay at the energies of interest (Hubbell and Seltzer, 2004). However, with compositional information and application of the proper attenuation coefficients, it would be possible to create a high-resolution density profile using the CT data.

The linear 2D X-ray images are relatively free from geometrical artifacts as they were collected as continuous scans using only the center of the X-ray cone beam. The TIFF images preserve the raw data as collected. The virtual slabbing correction of the JPG images assumes a round core of perfect geometry, so any deviation from a cylinder will create a corresponding dark or bright spot on the image. This correction can also create dark vertical lines near the edges of the image.

The X-ray CT data in the initial report data set have a number of artifacts which should not be mistaken for features in the core. Detailed processing of specific volumes could further minimize these artifacts.

Center of rotation artifacts: these artifacts are recognizable as a doubling of features, or an apparent wobble in the image (e.g., Chapter 4. Figure 4.4.13). Center of rotation artifacts appear because a single center point of rotation does not exist (for instance, the core tumbles within the liner or core is not held perfectly central in PCATS). Tumbling of core was more prevalent in this study than any other PCATS operation in the past, due to the undercut nature of the core.

CT montage artifacts: these artifacts are recognizable as lines in vertical slabs every ~6.7cm and are a result of the merging of two data sets. These artifacts can be exacerbated if the core moves even slightly in the liner between two rotations.

CT ring artifacts: these artifacts are recognizable as concentric rings in the CT TIFF stack (horizontal slices), or as vertical lines or repeated patterns in the CT JPG files (vertical slabs). They are particularly noticeable at the center of rotation (near the center of the core). Some of these ring artifacts were generated as sediment particles accumulated in the X-ray beam during the CT acquisition; this problem had not previously been observed in PCATS and will require protocol modifications to avoid similar issues in future.

All Linear 2D X-ray data can be found by hole in the expedition data directory under Physical Properties / Pressure Core / PCATS Linear Xray /. All CT data can be found in the same folder PCATS CT raw data /, PCATS CT slab images /, or PCATS CT slice images /.

Pressurized subsampling

Samples for further study under pressure were cut using PCATS. The core liner was cut with a rotating wheel, similar to a pipe cutter, and a guillotine blade was used to slice the sediment. Whenever possible, cuts were made at points where the core had already been fractured due to coring. Core was cut under pressure and cut pieces were transferred to storage chambers. Note that if the core sample is transferred under pressure and is the bottom sample taken from the cored section, then the core catcher will still be attached to the core liner. These chambers were then either rapidly depressurized, quantitatively depressurized (see 2.5 Quantitative Degassing), or stored at the University of Texas, Austin, for further analyses.

2.4.2 Depressurized Whole Core XCT

Depressurized whole-core was sent to Ohio State University for initial analysis. Whole core XCT was performed on a Samsung CereTom portable 8-slice XCT scanner. The scanner was used to collect CT images at a voxel resolution of 0.5mm by 0.5mm by 0.625 mm for cores up to 1.5 m long. The measurement is sensitive to the bulk density of the sample, but can also be affected by elements with a large atomic mass (for example, pyrite mineralization). The scans were used to identify features for further sampling and study and can be tied with bulk density measurements or bulk density log data.

All initial XCT data can be found by hole in the expedition data directory under Physical Properties / Depressurized Core / XCT /.

2.5 Quantitative Degassing

Quantitative degassing procedures were used to determine the concentration of hydrate on select samples.

Initial indication of the presence of hydrate can be seen from PCATS P-wave and density scans of the pressure cores. With this information, 0.33 to 3.3 ft (0.1 to 1.0 m) subsections of methane-hydrate bearing core were cut using PCATS. PCATS was used to transfer the sample into a 0.35 or 1.2 m storage

chamber, described above, which was then connected to a Geotek degassing/gas collection manifold (Figure 2.5.1 and Figure 2.5.2) to determine the total methane extracted from and initial concentration of hydrate within the core (Dickens et al., 2000). The degassing chamber is a simple 0.35 or 1.2 m aluminum or steel storage chamber and does not include any thermocouples or electrodes and cannot be imaged during depressurization. The depressurization occurred inside a temperature controlled room at $\sim 10^\circ\text{C}$ and in many cases included a residual DST in the chamber outside the core liner. Degassing of these sections was conducted over 2.5 to 142.5 hours depending on the section length, amount of hydrate present in the section, and scientific goals. Up to four degassing experiments could be run simultaneously with multiple apparatuses.

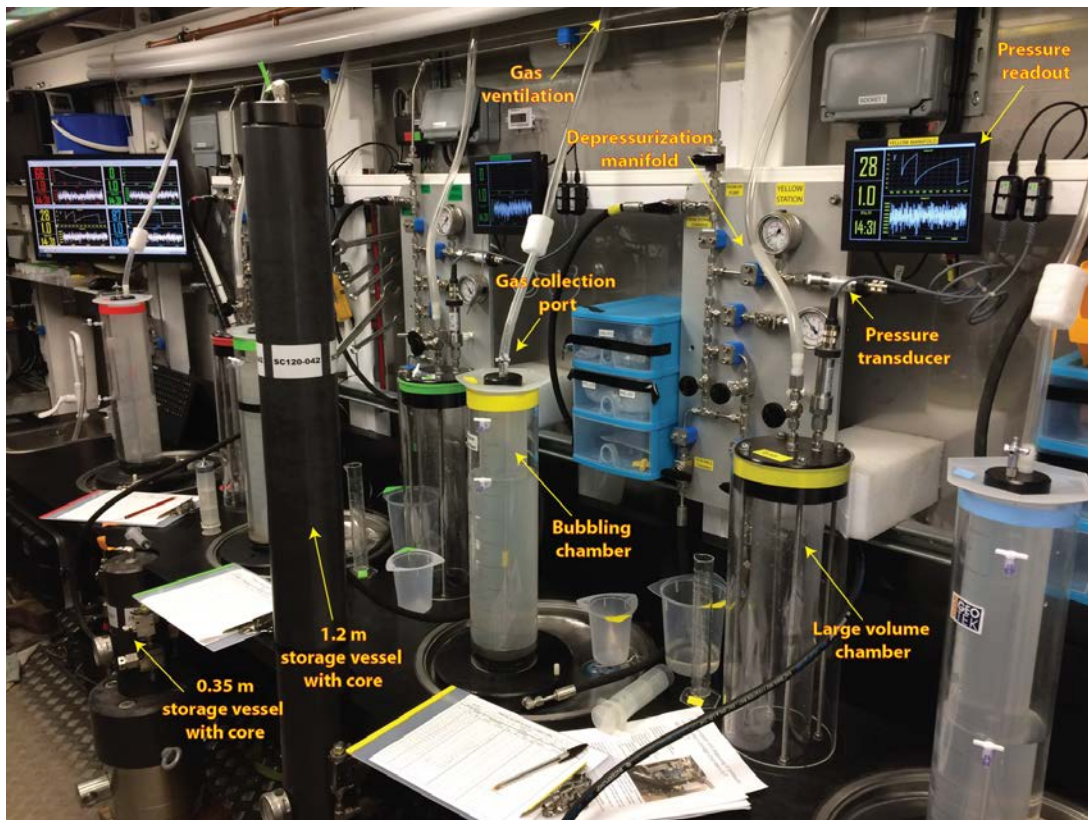


Figure 2.5.1 Photo of Geotek degassing manifolds and volume measuring equipment.

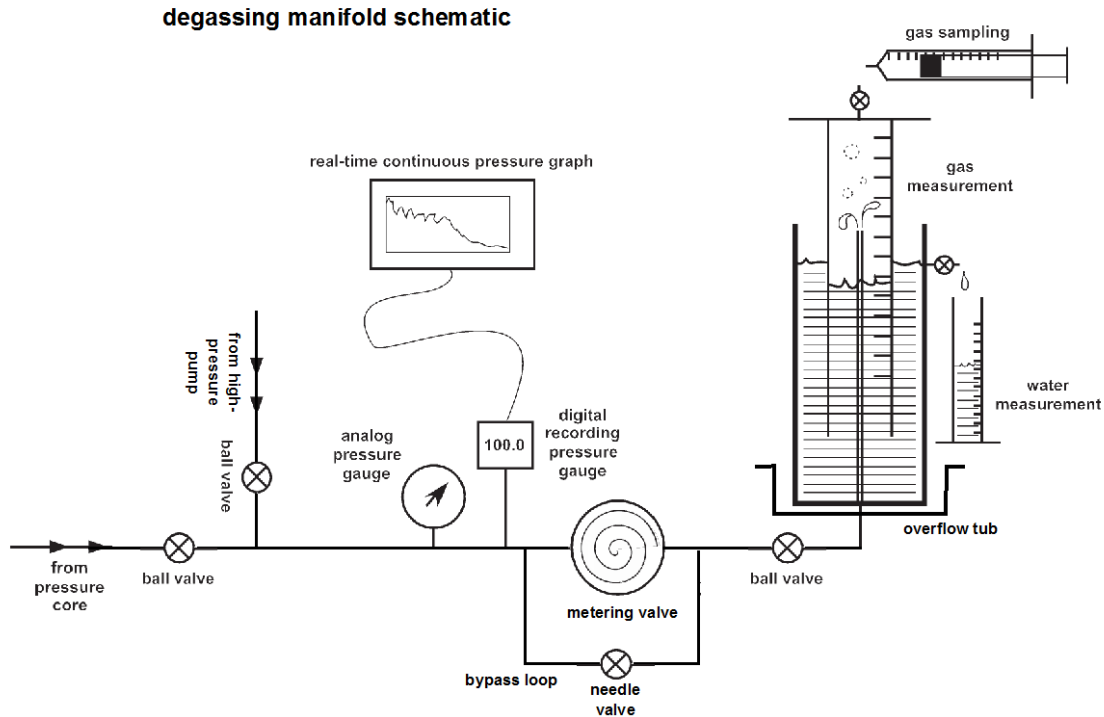


Figure 2.5.2 Schematic of Geotek degassing manifolds and volume measuring equipment.

During quantitative degassing the sample pressure was initially at approximately 20 MPa and was quickly depressurized to just above methane hydrate stability zone (about 8 MPa). Pressure was then instantaneously reduced step-wise by a small increment of pressure (0.1 to 1 MPa) and allowed to stabilize through hydrate dissociation. Gas that was forced out of the chamber during depressurization was collected in a gas trap constructed from an inverted 2 L graduated cylinder in a water column, and was measured, recorded, and sampled for compositional analysis. The volume of water forced out of the chamber was also measured and recorded to maintain an accurate mass balance. Alternatively, in some instances the gas was released to a large-volume chamber and in which the pressure up to 0.5 MPa was recorded.

After pressure had returned to a relatively stable condition, the process was repeated until the pressure in the chamber returned to atmospheric pressure. At the end of the experiment, the total amount of water forced from the chamber was added to the last gas increment as this is an accurate assessment of the gas remaining inside the chamber which could not escape. The contents of the chamber were removed intact in the liner if possible for curation, and the remainder of the sediment (and in some cases all of the sediment if completely disaggregated) was collected in plastic storage bags.

Methane hydrate saturation (S_h), the fraction of the pore volume that was filled with hydrate, was calculated using the total amount of methane collected in moles and the pore volume of the core section. The pore volume was calculated assuming a cylindrical core volume that completely fills the internal diameter of the core liner (5.08 cm) and the length of the section, with a porosity of 40%. An average porosity of 40% was assumed based on calculations from GC 955 H001 (H001) well logs (Boswell et al., 2012; Collett et al., 2012). Thermodynamic equilibrium was assumed. S_h reported from these

experiments represents a bulk saturation over the entire degassed section, and shorter intervals of higher or lower S_h may exist within the degassed section, suggested by variation in P-wave velocities. Quantitatively degassed sections can contain smaller-scale lithologic variation that influences S_h .

Gases collected from on-board degassing experiments were transferred to plastic syringes for onboard gas analysis (see 2.7 Geochemistry and Microbiology). Additional samples were collected in pre-evacuated copper tubes or steel gas cylinders for shore-based analysis. Gases collected in clamped copper tubes were shipped to Ohio State University for additional molecular and stable isotopic analyses to provide insight into the source of the gas (e.g. (Darrah et al., 2014; Whiticar, 1999)). Additionally, a subset of gases were collected in steel gas cylinders and shipped to CalTech for analysis of methane isotopologues to better understand methane sources (Stolper et al., 2014; Stolper et al., 2015)

All quantitative degassing data can be found by hole in the expedition data directory under Quantitative Degassing.

2.6 Lithostratigraphy

Lithostratigraphy was determined based on microscopic and macroscopic description of depressurized split cores, as well as X-ray images and physical properties of pressure cores. Visual core and smear slide descriptions were integrated with PCATS analyses to determine a set of lithofacies that provide an initial framework for interpreting the observed down core variation at a greater than cm-scale. Lithologic variation may occur on finer scales (mm-scale) within the described lithofacies, which will be further investigated beyond the scope of this report.

2.6.1 Lithostratigraphic nomenclature

We separately define Lithostratigraphic Units and lithofacies in sediments drilled at GC 955. Lithostratigraphic Unit is capitalized and lithofacies is lower case to conform to IODP style guides (IODP, 2012).

Lithostratigraphic Units contain packages of multiple lithofacies over the scale of tens to hundreds of meters. Lithostratigraphic Units are represented by Roman numerals that increase with depth

Lithofacies represent smaller packages of sediments with similar characteristics (average P-wave, gamma density, grain size) on the scale of centimeters to tens of centimeters. Lithofacies are not necessarily completely uniform and have observed laminations (generally finer than the scale of PCATS scanning), but represent a bulk change in sedimentological and physical properties on a map-able scale. Lithofacies are represented by numbers that increase with depth at the time of this initial interpretation.

2.6.2 Visual Core Description

Visual core descriptions (VCDs) are based on macroscopic and microscopic sediment type, sedimentary structures, and drilling disturbance. The techniques described below are similar to those used during ODP 204 (Shipboard Scientific Party, 2003), IODP 311 (Expedition 311 Scientists, 2006), NGHP-01 (Collett et al., 2008), and IODP 353 (Clemens and al., 2016).

All visual core description data can be found by hole in the expedition data directory under Lithostratigraphy / Visual Descriptions /.

Sediment classification

Sediment classification names reflect the composition and texture from visual description. Naming conventions generally follow the ODP sediment classification system of Mazzullo et al. (Mazzullo et al., 1988). A modified version of the Udden-Wentworth grain-size scale (Wentworth, 1922) was used to describe grain size (Figure 2.6.1). In this modified scale, clay describes grain size $<2\ \mu\text{m}$ rather than $<4\ \mu\text{m}$. Visual percentages were estimated based on the chart of Terry and Chilingar (Terry and Chilingar, 1955). Based on these percentages, the sediment was classified based on a system modified from Shepard (Shepard, 1954). Each sediment type is given a principal name preceded by adjective major modifiers ($>25\%$ of the sediment) and followed by minor modifiers (10-25% of the sediment), preceded by the word “with”. For example, unconsolidated siliciclastic sediment containing 50% silt, 30% sand, and 20% clay would be called sandy silt with clay. If the sediment is easily deformed by a finger, the sediment is named by grain size and no lithification term is added. Lithostratigraphic units were defined based on sediments of similar characteristics based on visual, smear slide, and PCATS observations.

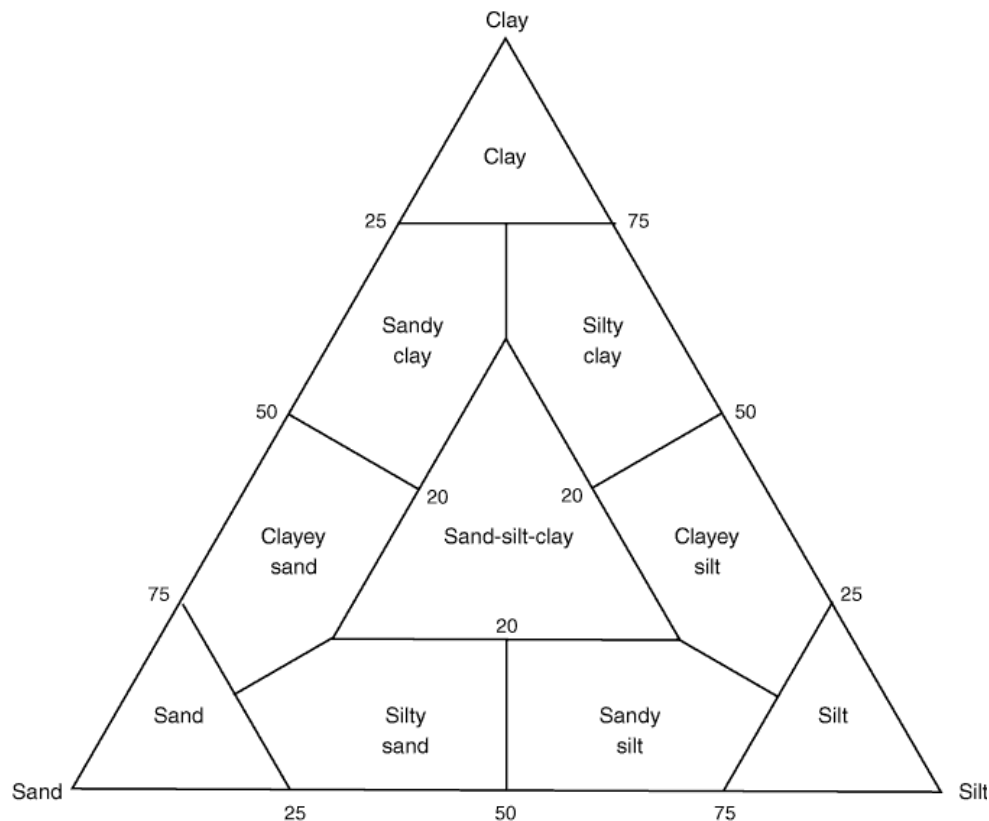


Figure 2.6.1 Shepard classification scale (Shepard, 1954). In our system, sand is defined as larger than $63\ \mu\text{m}$, and clay is defined smaller than $2\ \mu\text{m}$.

Sedimentary structures

Sedimentary structures formed by physical, chemical, and biological processes (e.g. grading, bioturbation, fossils, nodules, bedding, color banding) were described and entered in the VCDs. Structures suggestive of gas hydrate dissociation (soupy or mousse-like texture) were also noted. All contacts between lithologies are considered gradational and horizontal unless otherwise noted. Unless otherwise noted, all beds are considered non-graded. The bedding is assumed equal in thickness to described intervals of lithology, unless specifically described as containing beds/laminations of certain thickness. Bedding/laminations are classified as:

- <0.1 cm = very thin lamination,
- 0.1–0.3 cm = thin lamination,
- >0.3–0.6 cm = medium lamination,
- >0.6–1 cm = thick lamination,
- >1–3 cm = very thin bed,
- >3–10 cm = thin bed,
- >10–30 cm = medium bed,
- >30–100 cm = thick bed, and
- >100 cm = very thick bed.

Sediment color

Sediment colors of the split core surface were described using the Munsell Soil Color Chart (Munsell Color Company, 1994).

Core Photos

Photos of split whole round core were taken using a Canon EOS 7D. Adobe Photoshop was used to crop and adjust color and brightness.

All core photos can be found by hole in the expedition data directory under Lithostratigraphy / Core Photos /.

2.6.3 Smear slide description

Microscopic description of lithology was used to inform the sediment classifications. Small samples were collected by toothpick from split cores, smeared on a glass slide and dried on a hotplate. The slides were then covered with a drop of Norland optical cement and a glass cover slip, and then cured under a UV lamp.

These descriptions were used to characterize the presence and relative amount of lithogenic, biogenic, and authigenic sedimentary components. For each slide the percent of each observed component and grain size class was estimated. Major lithogenic minerals (e.g. quartz, clay mica, and feldspar) as well as major microfossil groups (foraminifera, radiolarians, diatoms, nannofossils) were identified and

abundance estimated. Organic matter/plant debris/lignite content was estimated, as well as authigenic precipitates such as carbonates and sulfides.

All smear slide data can be found by hole in the expedition data directory under Lithostratigraphy / Smear Slides /.

2.6.4 Laser diffraction particle size analysis

Grain size analysis was performed on small subsets (<1 cm³) of sample from depressurized core, either from quantitatively degassed core or pressure core that failed to hold pressure. These samples were disaggregated in a sodium hexametaphosphate solution before analysis on a Malvern Mastersizer 2000 particle size analyzer. The disaggregated sample was dispersed in freshwater within a 500 mL plastic beaker to obtain a laser obscuration rate between 10 and 20%. The standard operation procedure used in the particle size analyzer for these set of samples assumed a particle refractive index of 1.55, a particle absorption index of 0.1, and a dispersant refractive index of 1.33. The grain size distribution was recorded as a logarithmic set of 101 bins between 0.02 and 1400 µm. The standard output from the analyzer included 10th, 50th, and 90th percentile grain sizes, as well as volume-weighted and surface-weighted mean grain size. Due to the set bins in the software, 1.93 µm was used as the silt-clay boundary as the closest grain size bin to 2 µm.

All grain size data can be found by hole in the expedition data directory under Lithostratigraphy / Grain Size /.

2.6.5 Mineralogy

X-ray diffraction measurements were taken using a PANalytical X'Pert Pro Powder Diffractometer equipped with X'Celerator detector to determine the mineralogy. Preparation included drying and grinding 2 grams of sediment into a fine powder, and then the sample was back-loaded into a cavity mount. A beam of Cu K-alpha radiation with a wavelength of 0.15418 nm was directed at samples and the angles and intensities of diffractions off crystal faces were measured. This data was processed with Highscore Plus software to identify the minerals present based on diffraction peak patterns.

All mineralogy data can be found by hole in the data directory under Lithostratigraphy / XRD /.

2.7 Geochemistry and Microbiology

2.7.1 Pressure core gases

Field analysis – pressure core gases

Gas collected during depressurization of recovered pressure core samples (see 2.5 Quantitative Degassing) was analyzed using an Inficon Fusion MicroGC gas chromatograph with molecular sieve and PLOT Q columns and thermal conductivity detectors. Oxygen, nitrogen, methane, ethane, propane, butane, isobutane, isopentane, and pentane were measured. The detection limit for all gases was 10 ppmv; the quantification limit was 30 ppmv. Plastic syringes were used to collect and transfer gases.

Field sampling – pressure core gases

Additional gas samples were collected during quantitative degassing experiments for transport to shore-based labs at the Ohio State University and California Institute of Technology for additional analyses. These samples were collected either in 14 inches long by $\frac{3}{8}$ inch diameter copper tubes or 300 mL stainless steel cylinders that were evacuated and then connected to the bubbling chamber of the degassing apparatus.

All field gas analyses data can be found by hole in the data directory under Geochemistry / Gas /.

2.7.2 Sedimentary gases

Headspace gas samples were collected from approximately 1 to 2 depths per depressurized core, from a freshly cut section of core. These samples were collected as soon as depressurized core was available, between 30 minutes and several hours after depressurization, and collected from a fresh cut of the whole round core. These samples were collected adjacent to microbiology and pore water whole round samples. Two 2.5 cm³ sediment plugs were sampled from freshly opened core ends with plastic syringes immediately after depressurization. These plugs were extruded into 30 mL serum vials containing 5 mL of 1.0 M sodium hydroxide (NaOH). The serum vials were plugged with butyl rubber stoppers and capped with 20 mm aluminum crimp seals. The samples were shaken to mix sediment and NaOH, stored upside down, and then transported for post-cruise analysis to the University of Washington. New butyl stoppers were used to prevent contamination by absorbed methane (Magen et al., 2015).

2.7.3 Pore water

Due to space and personnel limitations, no pore water analyses were performed onboard the D/V *Q-4000*. Thus, the primary focus of on-board and dockside pore water efforts was the preservation of whole-round samples for post-cruise squeezing and analysis. While this approach prevents analysis of some time-sensitive pore water constituents (e.g. pH, alkalinity) many constituents can be measured weeks after collection when whole round samples are stored under an anoxic and refrigerated environment.

Field sampling – pore water

Whole round core samples between ~15 to ~20 cm in length were collected for pore water analysis from conventionalized core and from some sections processed through PCATS and quantitatively degassed. The core liner of these depressurized sections was pre-scored with a tubing cutter and then immediately placed within a glove box that was purged of ambient atmosphere and replaced by an anoxic ultra-high purity N₂ atmosphere to prevent oxidation of redox-sensitive elements. All further processing of the core occurred under N₂ atmosphere. The cutting of the liners was completed using a tubing cutter and split the sediment core with a sterilized spatula. The core was wrapped tightly in plastic wrap to prevent evaporation and was placed in a plastic bag and heat-sealed to retain the N₂ atmosphere during storage and transport. The sealed pore water whole rounds were stored refrigerated at 6 °C. These samples were shipped overnight in coolers with cold packs to the University of Washington.

Contamination control – pore water

The collected pore water samples had the potential to be contaminated by (1) drilling fluids during drilling and coring and (2) PCATS fluid during analysis and cutting of pressure cores. Due to time and laboratory limitations no tracers were added to mud tanks nor were micro-bead bags used during the expedition. Our approach to identify contamination by drilling fluid relied on comparison of pore water sulfate concentration to drilling fluid sulfate concentration then correcting for contamination based on the composition of the drilling fluid. The intervals recovered from coring (> 400 mbsf) were far below the typical depth of the sulfate-methane transition in the northern Gulf of Mexico 0 to 70 mbsf (Coffin et al., 2008; Expedition 308 Scientists, 2006a, b, c, d; Kastner et al., 2008; Paull et al., 2005; Pohlman et al., 2008; Presley and Stearns, 1986; Smith and Coffin, 2014), thus the presence of sulfate can be used as an indicator of contamination. To track PCATS water contamination, 1.9 g of cesium chloride was added to the ~150 L tanks that supply fresh water to PCATS to create a ~10 ppm concentration of cesium (Cs) in the PCATS fluid. Cs concentrations in seawater are low (~3 ppb) (Pilson, 2013) and is less readily absorbed by sediments with high ionic strength pore water (Flury et al., 2004) such as marine sediments.

To estimate mixing with contaminating fluids samples of drilling fluid were collected from the rig floor and PCATS water from the PCATS chamber for most cores. Each fluid sample was split into two 15 mL Nalgene bottles and one 8 mL glass vial. One 15 mL bottle was acidified with 0.05 mL of trace metal grade 16 N nitric acid. The final concentration of nitric acid in the 15 mL acidified sample was approximately 0.053 N. Each bottle was wrapped with Parafilm and stored and refrigerated at 6 °C.

Shore-based water collection

Whole round samples were shipped chilled with cold packs (not frozen) to the University of Washington for further processing and analysis, arriving in two batches on 31-May-2017 and 6-June-2017. Samples were immediately flushed with ultra-high purity nitrogen and stored at 4 °C for processing. Whole round samples were removed from the liner and the surface of the sediment scraped in a glove bag under N₂ atmosphere. The cleaned sediment samples were transferred to a Carver hydraulic press to extract pore water. Squeezed pore water was filtered through a pre-washed Whatman No. 1 filter and collected in cleaned plastic syringes. Waters collected in the syringes were further filtered with a 0.45 µm Gelman polysulfone disposable filter before analysis.

Sample allocation for specific analyses was determined based on the pore water volume recovered and analytical priorities with the analysis of pore water salinity, Cl, contamination tracer (Cs), O/H isotopes, SO₄, and the major cations being the highest priority. Sub-samples were preserved as follows: pore water subsamples for O/H analysis were stored in glass ampoules, in glass vials for analyses of halogens and ammonium, and in amber glass vials and subsequently frozen for Dissolved Organic Carbon (DOC) concentrations. In addition, pore water subsamples for sulfate concentration analyses were fixed with zinc-acetate and stored in centrifuge tubes, and samples for major element, minor element, and tracer (Cs) analysis were stored in plastic bottles and acidified with ultrapure nitric acid.

After analysis, pore water sub-samples were stored under appropriate conditions and available to the science party (Table 2.7.1). Likewise, the squeezed sediment split round cores were sectioned with one being stored at room-temperature and the other frozen, and made available to the science party.

| Analysis | O/H | DOC | Halogens and NH ₄ | SO ₄ | Cations | B and Si | Residue |
|----------------------------|----------------------|------------------------------|------------------------------|--|---------------------------------------|-----------------------------------|---------------------------------------|
| Subsample container | 1-2 ml glass ampoule | 1.5 ml amber screw top glass | 2ml screw top glass | 10 ml Corning plastic centrifuge tube; 0.1 ml sample from hal bottle to 9.9 ml Zn-acetate solution | 4 ml acid-cleaned plastic bottles | 4 ml acid-cleaned plastic bottles | 5 ml acid-cleaned plastic cryo-tubes |
| Treatment | No treatment | Frozen | No treatment | Zn-acetate | Acidified with 10 µL HNO ₃ | No treatment | Acidified with 10 µL HNO ₃ |

Table 2.7.1 Treatment and storage of squeezed pore water samples.

Initial analyses of salinity, chlorinity, and sulfate are reported for each hole in Chapter 3 and Chapter 4, with additional sample splits prepared for major/minor element, O/H isotope, and ammonium analyses.

Salinity

Salinity was determined with a Reichert temperature-compensated handheld refractometer with a precision of 0.5 practical salinity units (psu).

Chlorinity from titration with AgNO₃

Chlorinity (Cl) was determined via silver nitrate (AgNO₃) titration using a Metrohm Dosimat titrator with a precision of 0.2% based on repeated analysis of IAPSO standard seawater and a 50% dilution of IAPSO. Bromide (Br) and iodide (I) can be precipitated along with Cl. Dissolved Br concentrations (see Chloride, Bromide, and Sulfate from ion chromatography section below) can be used to correct the Cl concentrations for AgBr precipitation. In general, precipitation of AgBr contributes about 0.8 to 1.2 mM to the chlorinity concentration (~0.1-0.2%).

Chloride, Bromide, and Sulfate from ion chromatography

Chloride (Cl), bromide (Br), and sulfate (SO₄) were measured with a Metrohm 882 compact ion chromatograph (IC). Analytical precision was monitored by repeated analysis of four separate dilutions of IAPSO standard seawater that spanned the expected in situ concentration range. The precision of the

Cl, Br, and SO₄ analyses were 0.66%, 4.0%, and 0.8% respectively. Analytical accuracy was monitored by evaluation of four reference standards. The average percent difference between the known and measured concentrations for Cl, Br, and SO₄ were 1.0%, 4.0%, and 1.3%, respectively.

All pore water data can be found by hole in the data directory under Geochemistry / Pore Water /.

2.7.4 Microbiology

Field sampling -Microbiology

The primary goal of shipboard and dockside microbiology sampling was to collect and preserve whole round samples for DNA, 16S rRNA, and intact polar lipid analysis. Whole round microbiology samples (~15 cm) were collected from rapidly depressurized cores adjacent to and at the same time as pore water samples in the glove box (see Section 2.7.3 Pore water). The exterior of the core liner, sampling tools, and all surfaces in the glove box were sterilized with 70% isopropyl alcohol prior to sub-sampling. Each whole round was cut with a tubing cutter, then the sediment core was spit with a spatula. Each whole round was stored in a 710 mL sterile Whirl-Pak bag and immediately frozen at -20 °C. The samples were shipped from Port Fourchon to ExxonMobil labs in Annandale, NJ overnight in marine grade coolers with dry ice.

Contamination control - Microbiology

Microbiology samples are subject to the same contamination by drilling fluid and PCATS water as describe above for pore water samples. Characterization of the microbial communities present in drilling fluid via DNA and RNA can allow for assessing the degree of contamination by drilling fluid in core samples (Colwell et al., 2011; Lehman et al., 1995; Masui et al., 2008). To characterize the contaminating fluids samples of drilling fluid were collected from the rig floor and PCATS water from the opening of the PCATS chamber for approximately every core. Each fluid sample was collected in a sterile 50 mL centrifuge tube and immediately stored in a -20 °C freezer.

2.8 Wireline Logging

Downhole logs are measurements of physical, chemical, and structural properties of the formation surrounding a borehole that are made by sending probes in the borehole after completion of drilling. The data were rapidly collected, continuous with depth (sampled every 2.54mm to 15.24 cm), and measured in situ. Downhole logs are useful in calibrating the interpretation of geophysical data and provide a critical link for the integrated understanding of physical properties among different measurement scales. For UT-GOM2-1, where coring was not continuous, wireline logs provided the only way to characterize the formation between the cored intervals. They can be used to determine the actual thickness of individual units or lithologies when contacts are not recovered, to pinpoint the actual depth of features in cores with incomplete recovery, and to identify and characterize intervals that were not recovered.

Wireline logging operations during UT-GOM2-1 were conducted in H002. A logging tool string made of Schlumberger tools was lowered into the well to measure natural gamma radiation, formation resistivity, and hole deviation (see Figure 2.8.1 for an illustration of the tool string; see Table 2.8.1 and

Table 2.8.2; and tools description below for specifications of the tools and description of data channels, respectively).

In H005 a VES gyroscopic survey tool was deployed to determine the hole azimuth and deviation; no other downhole tools were deployed in H005.

2.8.1 Tools description

Detailed information on individual tools and their geological applications may be found in (Ellis and Singer, 2007; Goldberg, 1997; Rider, 1996; Schlumberger, 1991; Serra, 1984, 1986). A complete online list of acronyms for the Schlumberger tools and measurement curves is available at <http://www.apps.slb.com/cmd>.

Natural Gamma Ray

The Enhanced Digital Telemetry Cartridge (EDTC) provides high-speed (over 1 Mbps) communications between the wireline tools downhole and the acquisition system at the surface.

It includes also a sodium iodide scintillation detector to measure the total natural gamma ray emission of the formation, that can be used to characterize the lithology and to help match depths between the different logging passes. Total gamma ray counts are measured in American Petroleum Institute units (gAPI). When used in combination with a caliper log, such as provided by the HLDS (see below), the EDTC response to borehole size variations is corrected during acquisition using the caliper log.

Formation Resistivity

The High-Resolution Laterolog Array Tool (HRLA) provides six electrical resistivity measurements with different depths of investigation (including the borehole, or mud, resistivity and five measurements of formation resistivity with increasing penetration into the formation). The tool emits a focused current into the formation and measures the intensity necessary to maintain a constant drop in voltage across a fixed interval, providing direct resistivity measurements. The array has one central (source) electrode and six electrodes above and below it, which serve alternatively as focusing and returning current electrodes. By rapidly changing the role of these electrodes, a simultaneous resistivity measurement at six penetration depths is achieved. The tool is designed to ensure that all signals are measured at exactly the same time and tool position and to reduce the sensitivity to shoulder bed effects when crossing sharp beds thinner than the electrode spacing (Serra, 1984). The design of the HRLA, which eliminates the need for a surface reference electrode, improves formation resistivity evaluation compared to traditional dual induction and allows the full range of formation resistivity to be measured (e.g., <http://mlp.ldeo.columbia.edu/research/technology/schlumberger-wireline-tools-2/high-resolution-laterolog-array-tool-hrla/>).

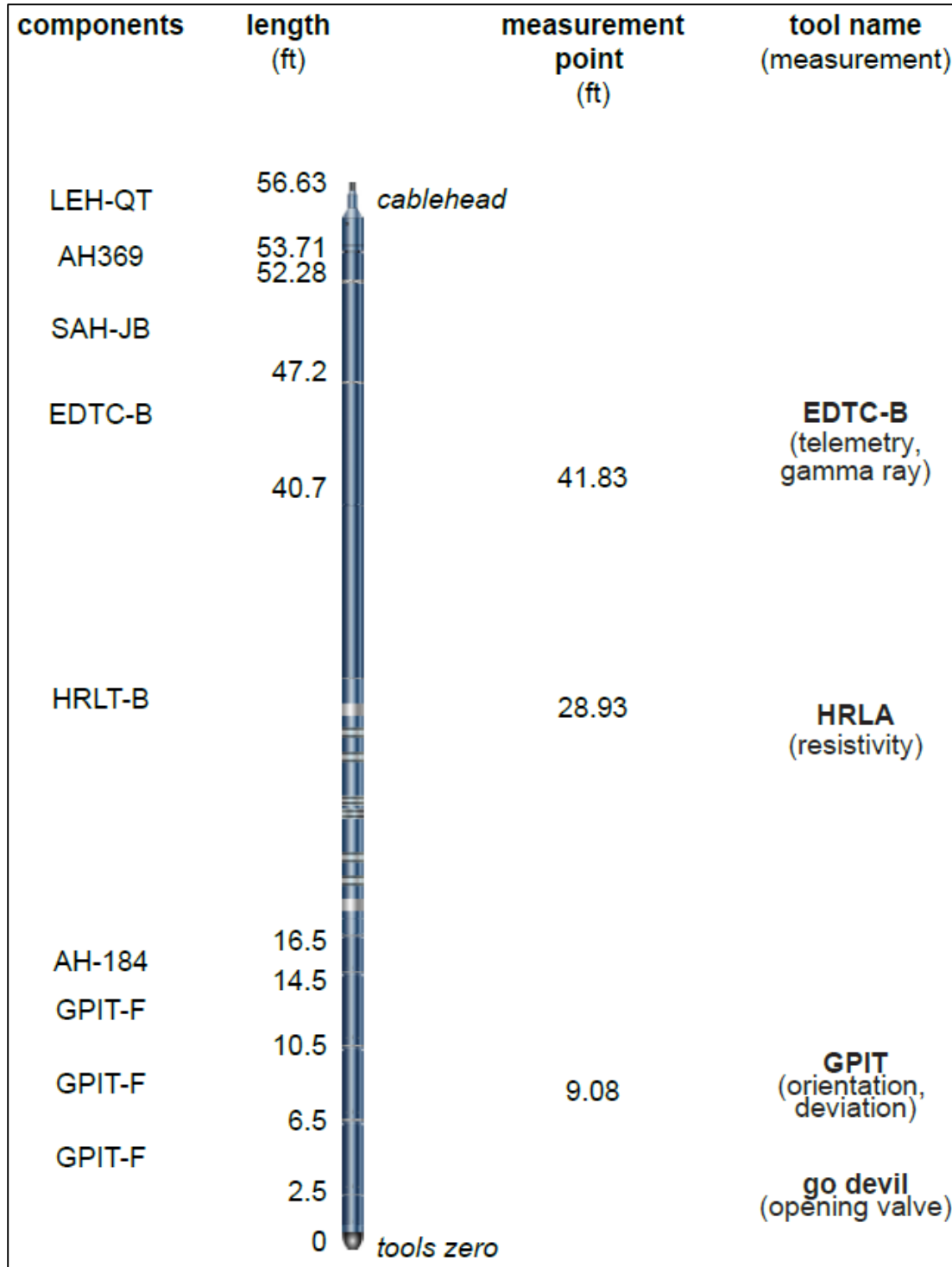


Figure 2.8.1 Wireline logging tool string deployed in Hole GC 955 H002.

| Tool | Measurement | Depth of Investigation (cm, approximate) | Vertical resolution (cm, approximate) |
|------|---|---|--|
| EDTC | Total gamma ray | 61 | 30 |
| HRLA | Resistivity | 127 (deepest) | 30 |
| GPIT | Orientation, deviation and acceleration | N/A | N/A |

Table 2.8.1 Logging tools used with Specifications.

| Tool | Output | Description | Unit |
|-------------|--|--|------------------|
| EDTC | GR | Enhanced Digital Telemetry Cartridge Total gamma ray | gAPI |
| | ECGR | Environmentally corrected gamma ray | gAPI |
| | EHGR | High-resolution environmentally corrected gamma ray | gAPI |
| HRLA | RLAx | High Resolution Laterolog Array Tool Apparent Resistivity from mode x (x from 1 to 5, shallow to deep) | Ωm |
| | RT | True Resistivity | Ωm |
| | MRES | Borehole fluid resistivity | Ωm |
| GPIT | DEVI | General purpose inclinometer tool Hole deviation | degrees |
| | HAZI | Hole azimuth | degrees |
| | F _x , F _y , F _z | Earth's magnetic field (three orthogonal components) | degrees |
| | A _x , A _y , A _z | Acceleration (three orthogonal components) | m/s ² |

Table 2.8.2 Acronyms and units used for downhole wireline tools, data, and measurements.

Borehole Deviation

In H002, the General Purpose Inclinometry Tool (GPIT) measured tool acceleration and orientation during logging. Tool orientation is defined by three parameters: tool deviation, tool azimuth, and relative bearing. The GPIT utilizes a three-axis accelerometer and a three-axis fluxgate magnetometer to record the orientation of the tool, which can be used to determine borehole inclination. In open hole intervals, the GPIT magnetometer records the magnetic field components (F_x , F_y , and F_z), and thus the borehole inclination and direction (azimuth) can be determined for a complete survey of the hole deviation. GPIT acceleration data (A_x , A_y , and A_z) also provide corrections for cable stretching and irregular tool motion, allowing a precise determination of log depths. Inside the pipe, the acquisition of GPIT data was configured to allow for the collection of a deviation survey. The GPIT sonde was located at the bottom of the tool string between two empty nonmagnetic GPIT housings to ensure the quality of the magnetic measurements in open hole (see Figure 2.8.1).

In H005, a VES survey international GS2 gyroscope tool was deployed independently on a non-electronic wireline to collect a survey of borehole deviation in compliance with U.S. government permitting regulations. The battery-operated tool records the magnetic orientation and depth in tool memory at pre-determined intervals. The data is downloaded after deployment when the tool returned to the rig floor.

Auxiliary Measurements

The Schlumberger Logging Equipment Head (LEH, or cable head) connects the logging tool string to the wireline and measures tension at the very top of the tool string. This tension is monitored continuously. Combined with the cable tension measured at the surface, it helps in diagnosing downhole operations while logging up or down in the borehole or when the tools are exiting or entering the drill pipe.

Because the logging tool string combines various components, it includes several adapters and joints between individual tools to allow communication, provide isolation, avoid interferences (mechanical, acoustic) or terminate wirings. These components are included in the tool string diagram shown in Figure 2.8.1.

2.8.2 Log Data Quality

The principal factor in the quality of log data is the condition of the borehole wall. If the borehole diameter varies over short intervals because of washouts or ledges, the logs measured by tools that require good contact with the borehole wall may be degraded. Deep investigation measurements such as gamma ray and resistivity, do not require contact with the borehole wall and are generally less sensitive to borehole conditions.

The accuracy of the logging depth depends on several factors. The depth of the measurements is determined from the measured length of the cable spooled out from the winch on the rig. Uncertainties in logging depth occur because of heave, cable stretch, cable slip or even tidal changes. Similar uncertainties occur with the drilling assembly and with the slickline that was used to recover the core samples during the marine test. All these factors can generate some depth discrepancy between core samples and logs, and between individual logging passes.

Logging data flow and processing

Data acquisition was monitored in real time and recorded using the Schlumberger field unit. Immediately after completion of logging operations, the data were handed to the on-board scientists for initial processing. First, a visually interactive program was used to match the depths of recognizable features across all the passes of the gamma ray log, used as a reference curve. After depth matching, all the logging depths were shifted to the seafloor based on an identified step in the gamma ray profile that is interpreted as the seafloor. The processed data were distributed to the scientific party in LAS and DLIS format.

2.9 References

- Boswell, R., Frye, M., Shelander, D., Shedd, W., McConnell, D. R., and Cook, A., 2012, Architecture of gas-hydrate-bearing sands from Walker Ridge 313, Green Canyon 955, and Alaminos Canyon 21: Northern deepwater Gulf of Mexico: *Marine and Petroleum Geology*, v. 34, no. 1, p. 134-149.
- Clemens, S. C., and al., e., 2016, Expedition 353 methods, Integrated Ocean Drilling Program.
- Coffin, R., Hamdan, L., Plummer, R., Smith, J., Gardner, J., Hagen, R., and Wood, W., 2008, Analysis of methane and sulfate flux in methane-charged sediments from the Mississippi Canyon, Gulf of Mexico: *Marine and Petroleum Geology*, v. 25, no. 9, p. 977-987.
- Collett, T., Riedel, M., Cochran, J., Boswell, R., Presley, J., Kumar, P., Sathe, A., Sethi, A., Lall, M., Sibal, V., and NE, S., 2008, Indian National Gas Hydrate Program Expedition 01 Initial Reports: New Delhi, India, USGS.
- Collett, T. S., Lee, M. W., Zyrianova, M. V., Mrozewski, S. A., Guerin, G., Cook, A. E., and Goldberg, D. S., 2012, Gulf of Mexico Gas Hydrate Joint Industry Project Leg II logging-while-drilling data acquisition and analysis: *Marine and Petroleum Geology*, v. 34, no. 1, p. 41-61.
- Colwell, F., Schwartz, A., and Briggs, B., 2011, Microbial community distribution in sediments from the Mount Elbert Gas Hydrate Stratigraphic Test Well, Alaska North Slope: *Marine and Petroleum Geology*, v. 28, no. 2, p. 404-410.
- Darrah, T. H., Vengosh, A., Jackson, R. B., Warner, N. R., and Poreda, R. J., 2014, Noble gases identify the mechanisms of fugitive gas contamination in drinking-water wells overlying the Marcellus and Barnett Shales: *Proceedings of the National Academy of Sciences*, v. 111, p. 14076-14081.
- Dickens, G. R., Wallace, P. J., Paull, C. K., and Borowski, W. S., 2000, Detection of methane gas hydrate in the pressure core sampler (PCS): volume-pressure-time relations during controlled degassing experiments: *Proceedings of the Ocean Drilling Program Scientific Results*, v. 164, p. 113-117.
- Ellis, D. V., and Singer, J. M., 2007, *Well Logging for Earth Scientists*, 2nd ed., Springer, 692 p.:
- Expedition 308 Scientists, 2006a, Site U1319, *in* Flemings, P. B., Behrmann, J. H., John, C. M., and the Expedition 308 Scientists, eds., *Proceedings of the Integrated Ocean Drilling Program, Volume 308: College Station TX* (Integrated Ocean Drilling Program Management International, Inc.).
- Expedition 308 Scientists, 2006b, Site U1320, *in* Flemings, P. B., Behrmann, J. H., John, C. M., and the Expedition 308 Scientists, eds., *Proceedings of the Integrated Ocean Drilling Program, Volume 308: College Station TX* (Integrated Ocean Drilling Program Management International, Inc.).
- Expedition 308 Scientists, 2006c, Site U1322, *in* Flemings, P. B., Behrmann, J. H., John, C. M., and the Expedition 308 Scientists, eds., *Proceedings of the Integrated Ocean Drilling Program, Volume 308: College Station TX* (Integrated Ocean Drilling Program Management International, Inc.).

- Expedition 308 Scientists, 2006d, Site U1324, *in* Flemings, P. B., Behrmann, J. H., John, C. M., and the Expedition 308 Scientists, eds., Proceedings of the Integrated Ocean Drilling Program, Volume 308: College Station TX (Integrated Ocean Drilling Program Management International, Inc.).
- Expedition 311 Scientists, 2006, Site U1328, *in* Riedel, M., Collett, T. S., Malone, M. J., and Expedition 311 Scientists, eds., Proceedings of the Integrated Ocean Drilling Program, Volume 311: Washington, DC (Integrated Ocean Drilling Program Management International, Inc.).
- Flemings, P. B., 2016, Y2Q1 Quarterly Research Performance Progress Report (Period ending 12/31/2015), Deepwater Methane Hydrate Characterization and Scientific Assessment, DOE Award No.: DE-FE0023919.
- Flury, M., Czigány, S., Chen, G., and Harsh, J. B., 2004, Cesium migration in saturated silica sand and Hanford sediments as impacted by ionic strength: *Journal of Contaminant Hydrology*, v. 71, p. 111-126.
- Goldberg, D., 1997, The role of downhole measurements in marine geology and geophysics: *Reviews of Geophysics*, v. 35, no. 3, p. 315-342.
- Hubbell, J. H., and Seltzer, S. M., 2004, Tables of X-Ray Mass Attenuation Coefficients and Mass Energy-Absorption Coefficients from 1 keV to 20 MeV for Elements Z = 1 to 92 and 48 Additional Substances of Dosimetric Interest, National Institute of Standards and Technology.
- Inada, N., and Yamamoto, K., 2015, Data report: Hybrid Pressure Coring System tool review and summary of recovery result from gas-hydrate related coring in the Nankai Project: *Marine and Petroleum Geology*, v. 66, Part 2, p. 323-345.
- Kastner, M., Claypool, G., and Robertson, G., 2008, Geochemical constraints on the origin of the pore fluids and gas hydrate distribution at Atwater Valley and Keathley Canyon, northern Gulf of Mexico: *Marine and Petroleum Geology*, v. 25, no. 9, p. 860-872.
- Lehman, R. M., Colwell, F. S., Ringelberg, D. B., and White, D. C., 1995, Combined microbial community-level analyses for quality assurance of terrestrial subsurface cores: *Journal of Microbiological Methods*, v. 22, no. 3, p. 263-281.
- Magen, C., Lapham, L., L., Pohlman, J. W., Marshall, K., Bosman, S., Casso, M., and Chanton, J. P., 2015, A simple headspace equilibration method for measuring dissolved methane: *Limnology and Oceanography: Methods*, v. 2015, no. 12, p. 637-650.
- Masui, N., Morono, Y., and Inagaki, F., 2008, Microbiological Assessment of Circulation Mud Fluids During the First Operation of Riser Drilling by the Deep-Earth Research Vessel Chikyu: *Geomicrobiology Journal*, v. 25, no. 6, p. 274-282.
- Mazzullo, J. M., Meyer, A., and Kidd, R. B., 1988, New sediment classification scheme for the Ocean Drilling Program, Handbook for shipboard sedimentologists, Technical Note No. 8, p. 45-67.

Munsell Color Company, I., 1994, Munsell Soil Color Chart (revised edition).

Paull, C. K., Ussler, W., Lorenson, T., Winters, W., and Dougherty, J., 2005, Geochemical constraints on the distribution of gas hydrates in the Gulf of Mexico: *Geo-Marine Letters*, v. 25, no. 5, p. 273-280.

Pilson, M. E. Q., 2013, *An Introduction to the Chemistry of the Sea*, Cambridge University Press, New York.

Pohlman, J. W., Ruppel, C., Hutchinson, D. R., Downer, R., and Coffin, R. B., 2008, Assessing sulfate reduction and methane cycling in a high salinity pore water system in the northern Gulf of Mexico: *Marine and Petroleum Geology*, v. 25, no. 9, p. 942-951.

Presley, B. J., and Stearns, S., 1986, Interstitial Water Chemistry, Deep Sea Drilling Project Leg 96, *in* Bouma, A. H., Coleman, J. M., Brooks, J., Bryant, W. R., Constans, R., Cremer, M., Droz, L. I., Ishizuka, T., Il, M. C. K., Kohl, B., Meyer, A. W., Normark, W. R., O'Connell, S., Parker, M., Pickering, K. T., Schroeder, C., Stelling, C. E., Stow, D. A. V., Sweet, W. E., Wetzel, A., and Whelan, J. K., eds., *Initial Reports of the Deep Sea Drilling Project 96: Washington (U.S. Government Printing Office)*, p. 697-709.

Rider, M., 1996, *The Geological Interpretation of Well Logs (2nd ed.)*: Caithness, Whittles Publishing.

Schlumberger, 1991, *Log Interpretation Principles/Applications: Houston (Schlumberger Educ. Services)*, SMP-7017, Schlumberger Educ. Services.

Schultheiss, P., Roberts, J., Druce, M., Priest, J. A., Holland, M., Yamamoto, K., and Yang, S., PCATS and PCATS Triaxial: Further Development and Recent Field Experience Making Core Measurements Under Pressure, *in* *Proceedings of the 8th International Conference on Gas Hydrates*, Beijing, China, July 29-Aug 2, 2014 2014.

Schultheiss, P. J., Holland, M., Roberts, J., Huggett, Q., Druce, M., and Fox, P., PCATS: Pressure Core Analysis and Transfer System, *in* *Proceedings 7th International Conference on Gas Hydrates*, Edinburgh, Scotland, United Kingdom, July 17- 21, 2011 2011, p. 10.

Serra, O., 1984, *Fundamentals of Well-log Interpretation: The interpretation of logging data (Vol. 1)*, Elsevier.

Serra, O., 1986, *Fundamentals of Well-log Interpretation: The interpretation of logging data (Vol 2.)*, Elsevier.

Shepard, F. P., 1954, Nomenclature based on sand-silt-clay ratios: *Journal of Sedimentary Petrology*, v. Vol. 24, p. 151-158.

Shipboard Scientific Party, Leg 204 summary, *in* *Proceedings of the Ocean Drilling Program, Initial Reports*, College Station, Ocean Drilling Program, 2003, Volume 204, p. 1-75.

- Smith, J., and Coffin, R., 2014, Methane Flux and Authigenic Carbonate in Shallow Sediments Overlying Methane Hydrate Bearing Strata in Alaminos Canyon, Gulf of Mexico: *Energies*, v. 7, no. 9, p. 6118.
- Stolper, D. A., Lawson, M., Davis, C. L., Ferreira, A. A., Neto, E. V. S., Ellis, G. S., Lewan, M. D., Martini, A. M., Tang, Y., Schoell, M., Sessions, A. L., and Eiler, J. M., 2014, Formation temperatures of thermogenic and biogenic methane: *Science*, v. 344, no. 6191, p. 1500-1503.
- Stolper, D. A., Martini, A. M., Clog, M., Douglas, P. M., Shusta, S. S., Valentine, D. L., Sessions, A. L., and Eiler, J. M., 2015, Distinguishing and understanding thermogenic and biogenic sources of methane using multiply substituted isotopologues: *Geochimica et Cosmochimica Acta*, v. 161, p. 219-247.
- Terry, R. D., and Chilingar, G. V., 1955, Summary of "Concerning some additional aids in studying sedimentary formations" by M.S. Shvetsov: *Journal of Sedimentary Petrology*, v. 25, p. 229–234.
- Wentworth, C. K., 1922, A scale of grade and class terms of clastic sediments: *Journal of Geology*, v. 30, p. 377-392.
- Whiticar, M. J., 1999, Carbon and hydrogen isotope systematics of bacterial formation and oxidation of methane: *Chemical Geology*, v. 161, no. 1–3, p. 291-314.